

MICROCOPY RESOLUTION TEST CHART  
NATIONAL BUREAU OF STANDARDS-1963-A

AD-A176 973

THE RELATIONSHIP BETWEEN  
 PERMANENT REMANENT DEMAGNETIZATION  
 AND STRESS IN CRYSTALLINE ROCKS

Approved for public release;  
distribution unlimited.

AIR FORCE OFFICE OF SCIENTIFIC RESEARCH (AFSC)  
 NOTICE OF TRANSMITTAL TO DTIC  
 This technical report has been reviewed and is  
 approved for public release IAW AFR 190-12.  
 Distribution is unlimited.  
 MATTHEW J. KUTNER  
 Chief, Technical Information Division

DTIC FILE COPY

NER *New England Research*

DTIC  
 ELEC  
 FEB 24 1987  
 S  
 D

REPORT DOCUMENTATION PAGE

1a. REPORT SECURITY CLASSIFICATION <b>Unclassified</b>		1b. RESTRICTIVE MARKINGS	
2a. SECURITY CLASSIFICATION AUTHORITY		3. DISTRIBUTION/AVAILABILITY OF REPORT Approved for Public Release; Distributed Unlimited.	
2b. DECLASSIFICATION/DOWNGRADING SCHEDULE		4. PERFORMING ORGANIZATION REPORT NUMBER(S)	
4. PERFORMING ORGANIZATION REPORT NUMBER(S)		5. MONITORING ORGANIZATION REPORT NUMBER(S) <b>AFOSR-TR- 87-0110</b>	
6a. NAME OF PERFORMING ORGANIZATION Applied Research Associates New England Div.	6b. OFFICE SYMBOL (If applicable)	7a. NAME OF MONITORING ORGANIZATION <b>AFOSR</b>	
6c. ADDRESS (City, State and ZIP Code) South Royalton, VT 05068		7b. ADDRESS (City, State and ZIP Code) <del>Wash DC</del> Bolling AFB, DC 20332	
8a. NAME OF FUNDING/SPONSORING ORGANIZATION Air Force Office of Scientific Research	8b. OFFICE SYMBOL (If applicable) AFOSR/NA	9. PROCUREMENT INSTRUMENT IDENTIFICATION NUMBER F-49620-85-C-0135	
8c. ADDRESS (City, State and ZIP Code) Bolling AFB, DC 20332-6448		10. SOURCE OF FUNDING NOS.	
		PROGRAM ELEMENT NO.	PROJECT NO.
		TASK NO.	WORK UNIT NO.
11. TITLE (Include Security Classification) The Relationship Between Permanent Remanent Demagnetization and Stress in Crystalline Rocks		61102	2302 C1
12. PERSONAL AUTHOR(S) Randolph Martin, III			
13a. TYPE OF REPORT Annual Report	13b. TIME COVERED FROM 1Sept85 TO Aug3186	14. DATE OF REPORT (Yr., Mo., Day) October 30 1986	15. PAGE COUNT 50
16. SUPPLEMENTARY NOTATION			
17. COSATI CODES		18. SUBJECT TERMS (Continue on reverse if necessary and identify by block number)	
FIELD	GROUP	Demagnetization; Stress in Rocks; Measuerment Techniques	
	SUB. GR.		
19. ABSTRACT (Continue on reverse if necessary and identify by block number) See Attached Abstract			
20. DISTRIBUTION/AVAILABILITY OF ABSTRACT UNCLASSIFIED/UNLIMITED <input checked="" type="checkbox"/> SAME AS RPT. <input type="checkbox"/> DTIC USERS <input type="checkbox"/>		21. ABSTRACT SECURITY CLASSIFICATION Unclassified	
22a. NAME OF RESPONSIBLE INDIVIDUAL Dr. Spencer T Wu		22b. TELEPHONE NUMBER (Include Area Code) 202/767-4935	22c. OFFICE SYMBOL AFOSR/NA

## ABSTRACT

A suite of experiments has been initiated to study the effect of a generalized state of stress on the thermoremanent magnetization (TRM) of rocks. Several laboratory investigations have shown that the application of stress results in the permanent reduction in remanent intensity, and that the magnitude of the change is proportional to the peak stress experienced by the material. This property seemed ideally suited for use as the sensing element in a passive piezometer. The concept was successfully demonstrated on the HE shot, ONE TON. Magnetized rock cores were embedded in the grout at various distances from the working point. The stresses inferred from the demagnetization of the cores recovered after the shot were in excellent agreement with those predicted by empirical stress attenuation curves.

Based on the ONE TON results, a detailed study of the factors that control the magnitude of permanent stress-dominated magnetic changes was warranted. Specifically, we are examining (i) the effect of initial remanent intensity on the decrease in magnetization per increment of applied load, (ii) the influence of chemical composition and grain diameter of the magnetic grains on the total piezomagnetic effect, (iii) the difference between hydrostatic and non-hydrostatic loading on the reduction of remanent magnetization and (iv) the effect of the orientation of the magnetic vector with respect to the greatest principal stress direction on the total piezomagnetic phenomena.

Experiments have been conducted on a gabbro and a diabase in which the remanent magnetization was controlled by pseudo-single-domain titanomagnetite grains. All the test were carried out on samples that had thermoremanent moments induced in fields ranging from 3 to 100 Oe. The results to date indicate that (i) differential stress produces a larger piezomagnetic effect the hydrostatic pressure over the same stress range, (ii) the piezomagnetic effect increases with increasing initial intensity and (iii) the permanent change in magnetization per stress increment is greater at low stress (less than 500 bars) than at high stress levels.

(2)

DTIC  
ELECTE  
FEB 24 1987  
S D

THE RELATIONSHIP BETWEEN  
PERMANENT REMANENT DEMAGNETIZATION  
AND STRESS IN CRYSTALLINE ROCKS

Government Prime Contract No.  
AFSC F 49620-85-C-0135  
Applied Research Associates, Inc.  
Albuquerque, NM

Air Force Office of Scientific Research  
Bolling Air Force Base  
Washington, D. C.

October 30, 1986

Prepared by

This document has been approved  
for public release and sale; its  
distribution is unlimited.

Randolph J. Martin, III  
James S. Noel  
New England Research, Inc.  
P. O. Box 857  
Norwich, Vermont 05055



## INTRODUCTION

For decades scientists have explored a wide variety of techniques to accurately measure changes in the local stress field due to impulsive and shock loading. Ideally, the most effective approach is to detect changes in a physical property of the material experiencing the loading that is uniquely related to stress. For example, in an elastic material, (below the yield point) stress is a single valued function of strain. Quite simply, then, by measuring change in strain, the corresponding change in stress can be readily computed. While this approach works well for most metals and ceramics, naturally occurring soils and rocks present a more arduous task. The most obvious difficulty is that strain is as much a function of loading path as is stress. Furthermore, most of the other physical properties of soils and rocks that can be readily determined lead to equivocal results when used to infer stress changes.

The most common method of measuring in situ stress changes is to embed a device in the host material whose output is proportional to stress. One type of piezometer consists of a piezoresistive element mounted on a diaphragm or plate immersed in an encapsulated fluid chamber. When the host material deforms, the pressure in the fluid chamber increases and changes the resistance of the sensing element. When suitably calibrated, the change in resistance can be directly correlated with the mean stress change in the material undergoing dynamic loading. During the application of dynamic load, these sensors yield not only the stress but the stress-time history as well. The measurement seems straightforward in principle, but the reality of the situation is certainly more complicated. First, the host material is not homogeneous but contains bedding planes, joints and faults. These planar discontinuities serve as locii for deformation and produce large scale displacement and block motion. Such motion reduces the success rate of experiments fielded on the test. In most instances, the instruments survive the high acceleration and stress; but the cables connecting the sensing device to the recording system are often severed, and consequently the information from the sensor is lost. If the success rate

for active instrumentation is controlled by the survivability of the cable, it would be prudent to field passive experiments not only to corroborate the results obtained on the active instruments but also to insure some reliable data in the event of a low recovery rate for the active experiments.

Some measurements, unfortunately, cannot be made passively. For example, time of arrival of the shock front and its rise time can only be obtained with active instrumentation. However, the peak stress and deformation associated with the shock front can certainly be measured passively. The maximum stress experienced by the material can be determined by detecting a stress sensitive change in some physical property of an inclusion in the host material. One technique that has been successfully applied is to simply use materials that have been observed to undergo stable phase changes at a fixed pressure. By utilizing several materials with well characterized phase changes over the range of pressures anticipated during detonation of the device, an estimate of the peak pressure can be obtained for a number of positions. This technique is limited by the fact that it only gives a lower bound on the stress at any point. If the stress is significantly greater than that required to drive the reaction, the information is not recoverable. Another possibility is to deploy a single material with a property that varies monotonically with stress over the range of interest. Laboratory studies on rocks with pseudo-single domain titanomagnetite grains have shown that during initial loading, a permanent decrease in the remanent magnetization occurs. This decrease is greatest when the orientation of the magnetic moment and the greatest principal stress are coincident. Furthermore, the magnitude of the permanent demagnetization is directly proportional to the peak stress experienced by the rock. (Martin & Wyss, 1975). In light of this observation it seemed worthwhile to see if this phenomena could be successfully applied to the measurement of peak stress on several underground tests. It was of particular interest not only to measure the peak stress as a function of range but also to determine if the severe environment in the vicinity of the working point would detract from the applicability of the technique at high stress levels. With these questions in mind, experiments were fielded on MINI JADE and the HE shot ONE TON.

## BACKGROUND

Many investigators have observed changes in rock magnetization due to application of stress (*Ohnaha and Kinoshita, 1968; Nagata, 1969; Nagata and Carleton, 1969; Ohnaha, 1969; Martin and Wyss, 1975; Jelenska, 1975; Kean et al., 1976; Martin et al., 1976; Martin, 1980*). The total magnetization of a rock is the vectorial sum of the remanent magnetization and the induced magnetization. The remanent magnetization is the magnetization a material possesses in the absence of an external field, whereas the induced magnetization is proportional to the applied field. Both remanent and induced magnetization change with applied stress, but only the induced magnetization is totally recoverable. When a rock with a remanent moment is initially loaded in compression, it begins to demagnetize; however, upon unloading the magnetization does not return to its initial value but exhibits a permanent demagnetization. The magnitude of change at the termination of the stress cycle is a function of the maximum stress that the specimen experienced, the intensity of the remanent moment, the magnetic grain size and the orientation of the magnetic vector with respect to the greatest principal stress direction.

*Martin and Wyss (1975)* observed that when a sample was loaded cyclically in compression with the peak stress augmented for each cycle, the total magnetization of the specimen at the termination of each loading cycle decreased. This result is shown in Figure 1 for a gabbro sample from Rapidan, Virginia, loaded cyclically in uniaxial compression. The magnetization parallel to the loading axis is plotted as a function of stress. The remanent vector for this sample was parallel to the loading axis. Stress cycling continually reduced the zero stress value of remanent magnetization. In a very real sense then the piezomagnetic effect reported in this study demonstrated the potential of remanent magnetization as a means of measuring the peak stress developed in the material. Quite simply, if the initial and final magnetization of a rock sample were known, a calibration similar to that in Figure 1 could be carried out and the peak stress that the rock has experienced readily determined.

After many additional tests the approach outlined above seems to hold up for a wide range of physical conditions. First, the piezomagnetic effect is not pronounced in rocks with pseudo single domain and multidomain magnetic grains with a high titanium content. The titanomagnetite grains that exhibit the optimum piezomagnetic effect have mean diameters between 10 and 20 microns and a Curie temperature of near 550°K. The piezomagnetic effect is controlled by movement of the domain walls within the magnetic minerals. On the first loading cycle the movement of the domain walls has a large irreversible component (*Boyd et al., 1984*). Subsequent stress excursions to the same or lower level yield reversible domain wall motion. Second, the optimum piezomagnetic effect is observed when the greatest principal stress direction and the remanent moment are coincident or do not differ by more than 15° for five kilobars of stress. Rotation is typically away from the greatest principal stress direction. Finally, *Pike et al., 1981* noted that the demagnetization described above cannot distinguish between pressure and differential stress: it appears to respond to the total stress that has been applied to the material.

Since the remanent magnetization of some igneous rocks is permanently altered when initially stressed and the change in magnetization is directly proportional to the magnitude of the applied stress, these particular rocks are well suited for use as piezometers. In light of this fact, rock cores with known physical and magnetic properties were placed at various distances from the working point on MINI JADE and ONE TON.

After the test, the samples were retrieved from ONE TON; the samples from MINI JADE are still in place. Nearly all the samples were recovered intact. Next, the permanent demagnetization of each sample was computed (Figure 2). The magnitude of the change in remanent intensity was then correlated with the stress required to produce the same amount of demagnetization in laboratory samples of the same rock type (Figure 3). In this way, the peak stress developed by the charge was obtained as a function of range (Figure 4).

Samples on ONE TON were fielded at ranges of 6.0, 6.5, 7.5, 11.0, 13.0, 16.5, and 23.5 feet. At a distance of 6.0 feet, a peak stress of 10 kb was inferred and at 6.5 feet, a stress of 9.2 kb was observed. Stresses of 2.0, 1.3, 0.9 and 0.3 kb were measured at distances of 11, 13.5, 16 and 23.5 feet respectively. These measurements are in very good agreement with the empirical equation relating peak stress to range which is used by Sandia National Laboratories (Figure 5). Based on the results obtained on ONE TON, the potential of piezomagnetism as a passive stress gage has been successfully demonstrated. The successful ONE TON experiment is very encouraging. The results indicate that the piezomagnetic response of rock cores can provide an inexpensive and reliable method of measuring the peak mean stress developed during shock loading.

In spite of the research that we have carried out on piezomagnetism over the past eight years there are a number of critical questions that must be resolved as piezomagnetic sensors are fielded. Gaps in our understanding persist because most of the theoretical and laboratory studies examining the effect of stress on rock magnetism have not considered the permanent demagnetization due to initial loading but have addressed instead multi-cycle behavior where the magnetic intensity is reproducible, if not reversible, from cycle to cycle. The reason for this approach is a direct consequence of the problem under investigation; in this case, earthquake processes. Since earthquakes occur on pre-existing faults, it is clear that such regions have undergone repeated stress cycles. In this context, the initial loading is not of primary importance and has not been extensively studied.

A number of fundamental gaps persist in our understanding of piezomagnetism. For example, it is of interest to know if the stress sensitivity increases with increasing initial magnetic intensity. Furthermore, what is the optimum titanomagnetic composition and grain size for the piezomagnetic effect? Can permanent changes in rock

magnetism due to differential stress be separated from those due to hydrostatic loading? What happens when the remanent magnetic vector is not parallel to the greatest principal stress direction; can the rotation of the magnetic vector be used to infer principal stress directions as well as the magnitude of the stresses? With these questions in mind, a program was initiated aimed at resolving these topics and placing a stronger scientific foundation under the piezomagnetic response of rocks.

#### EXPERIMENTAL RESULTS

In order to conduct meaningful piezomagnetic experiments on a rock with a significant percentage of titanomagnetite grains, the magnetic mineralogy must be well characterized. The magnetic properties of five rock types considered as potentially suitable for piezomagnetic studies are given in Table I. These five rock types, a gabbro (Rapidan, VA), the Ralston diabase (Golden, CO), a basalt (Dotzero, CO), a granite (Westerly, RI) and an andesite (Mt. St. Helen's, WA) were initially selected for two important reasons. First, other investigators have used these rocks in previous studies (other than piezomagnetism); consequently there was existing data base for these rocks. Second, homogeneous blocks of each rock could be readily obtained without too much field time.

In Table I the magnetic susceptibility, the coercivity, the Curie temperature, the saturation magnetization and the grain size for each of the five rocks is given. The *magnetic susceptibility* is the ratio of the observed magnetization to the applied magnetic field. As the field strength increases the magnetization of the material increases with the susceptibility serving as a proportionality constant. At low field strengths, up to 100 Oe, the relationship between applied field and induced magnetization is linear and consequently, the magnetic susceptibility is treated as a constant.

The *coercivity* is a measure of resistance to movement of the domain walls of the magnetic minerals. When a specimen is alternately driven to magnetic saturation in a positive and then a negative field, hysteresis is

prominent. The value of the magnetic field at which the total magnetic induction, B, decreases to zero is termed the coercivity.  $B = H + 4\pi J$  where H is the applied magnetic field and J is the magnetization of the rock.

The *Curie temperature* is the temperature at which the remanent magnetization drops to zero: i.e. the domains in the magnetic grains are randomly oriented. It has been shown that the Curie temperature is an excellent indicator of composition of titanomagnetite grains. Figure 6 gives the change in magnetization with increasing temperature for Rapidan gabbro. The magnetization decreases nearly linearly with increasing temperature up to 750°K and then rapidly decreasing to several tenths of an emu/g at 850°K. The temperature at which the magnetization perceptibly decreases is reported as the Curie temperature.

The Curie temperatures of all five rock types were very close, varying between 530 and 580°C. This indicates that the composition of the magnetic grains are similar. Titanomagnetite form a solid solution series with end members of Fe:TiO<sub>2</sub> magnetite, (Curie temperature 120°C) and Fe<sub>2</sub>O<sub>3</sub> ulvöspinel, (Curie temperature 580°C). As the composition moves from pure magnetite to ulvöspinel, the Curie temperature decreases linearly with increasing titanium content. Based on the Curie temperatures observed on the five rock types listed in Table I, the composition of magnetic mineralogy is almost pure magnetite; only the magnetic carriers in the diabase contain a significant amount of titanium.

The *saturation magnetization* is the maximum magnetization that the sample acquired in an applied field of 15,000 Oe. Typically about 50 percent of the saturation magnetization develop with the application of a field of several hundred Oersted (Oe). The magnetic saturation reported is for the bulk sample, an aggregate of silicate minerals and titanomagnetite grains. For comparison, the saturation magnetization of iron (Fe) is 218 emu/g and for single crystal magnetite (Fe<sub>3</sub>O<sub>4</sub>) is

92 emu g. Since the magnetic minerals constitute between 2 and 6 percent of the rocks by volume, saturation magnetization in the vicinity, several emu g are reasonable.

One of the most important characteristics of rocks exhibiting a piezomagnetic effect is the presence of pseudo-single-domain magnetic grains. Magnetic grains can be conveniently described as either single domain, pseudo single domain or multidomain. For a fixed composition titanomagnetite, as the grain size increases from 0.1 to 200 microns several pronounced changes occur: the number of domains increases, the coercivity decreases and the stability of the remanence decreases. For magnetite, single domain behavior is observed when the mean diameter is between 0.1 and 5 microns (*Dunlop, 1973; Day, 1973*). The transition from pseudo single domain to multidomain grains occurs at grain sizes of 15 to 40 microns. Single domain ( $10^3$  Oe) and stable or hard remanence. Multidomain grains exhibit low coercivities (several tens of Oe) and unstable or soft remanence. Pseudo-single-domain magnetization is observed in grains 1-30 microns and in size is characterized by coercivities of 160 Oe or so. Pseudo single domain grains are the stable carriers of the remanent moment. They remain largely unaffected by small changes in field strength (at temperatures well below the Curie temperature) but are responsible for the most reproducible piezomagnetic effects (*Nagata and Carleton, 1969; Ohnaka, 1969, Kean et al., 1976, Martin et al., 1976*).

The five rocks listed in Table I all possess pseudo-single-domain grains. The magnetization of the basalt and andesite is most certainly controlled by pseudo-single-domain magnetic minerals. The diabase, gabbro and granite contain pseudo-single-domain as well as multidomain titanomagnetite grains. This can be inferred from the distribution of magnetic grain diameters and the somewhat low coercivities of 42 and 47.5 Oe for the granite and gabbro respectively. The coercivity of the diabase is reported as nearly zero Oersteds. This is anomalously low and consequently the value is suspect. The determination of coercivity and

saturation magnetization were made in facilities developed by L. N. Mulay at the College of Earth and Mineral Sciences, The Pennsylvania State University, University Park, Pennsylvania. An independent determination of these values is being carried out by Prof. Edwin Larson, Department of Geology, University of Colorado, Boulder, Colorado.

Of the five rocks listed in Table I only three appear well suited for this study, the basalt, the gabbro and the diabase. All three have pseudo-single-domain grains, and a high saturation magnetization. Since one key aspect of this study is to examine the influence of remanent intensity on the piezomagnetic effect, a large saturation moment was essential.

The composition of all the material studied during the first year was restricted to rocks in the titanomagnetite solid solution series. These oxides most commonly occur uniformly dispersed in igneous rocks. Their ready accessibility in a naturally occurring *ceramic type* host made them ideally suited for study. Another magnetic mineral, pyrrhotite,  $Fe_7S_8$ , possesses characteristics that indicate it may also exhibit a piezomagnetic effect. It is *ferrimagnetic*, as is the titanomagnetite series, and has exhibited pseudo-single-domain behavior in a domain structure study carried out by *Halgedahl and Fuller, (1983)*. Unfortunately pyrrhotite is a sulfide ore and is not found uniformly dispersed in a relatively homogeneous host. During the second year of this study pseudo-single-domain pyrrhotite grains will be incorporated into a composite and their piezomagnetic effect examined.

Piezomagnetic experiments have been conducted on the diabase and gabbro. Specimens are currently being prepared from the Dotzero basalt and will be studied in the next few months. Specifically it was of interest to know how the magnitude of the piezomagnetic effect depended on the initial remanent intensity and the mode of deformation. In most studies of remanent magnetism in rocks, the intensity developed as the rock cools through the Curie point in 0.5 Oe field (the Earth's magnetic field) is of

most interest. However, when the rocks will be used as piezomagnetic sensors, it is logical to ask if increasing the initial remanent intensity will increase the stress sensitivity? For example, the gabbro samples deployed on ONE TON had an initial magnetic intensity of  $3.0 \times 10^{-2}$  emu/cm<sup>3</sup>. The saturation magnetization for that material is a factor of 50 greater than that developed in the ONE TON samples. Is the piezomagnetic change greater when the remanent moment was larger? Does hydrostatic loading produce the same change per increment of stress as non hydrostatic loading? In order to answer these questions, rock cores were prepared in a uniform manner with varying remanent intensities and then stressed in a field free, non magnetic deformation test apparatus.

The rock specimens were ground, right circular cylinders 4.13 cm in length and 1.79 cm in diameter cored from large blocks of diabase, gabbro and basalt. Then, a thermoemant magnetization (TRM) was developed in each sample. First, the sample was heated to 600°C, a temperature well above the Curie temperature. The specimens were heated in a furnace fitted into a two layer mu-metal shield which reduced the magnetic field inside the shield to less than 100 gammas (nT). The furnace coils were non-inductively wound to avoid generating a magnetic field when the furnace was in operation. After the sample reached 600°C the furnace was turned off; simultaneously, two Helmholtz coils surrounding the furnace, but inside the mu-metal shield, were energized to magnetize the rock as they cooled through their Curie temperature. The coils had a radius of 8.89 cm and were separated by 8.89 cm. Each coil consisted of 371 turns of No. 22 copper magnet wire. Helmholtz coils generate a very uniform magnetic field along the axis of a two coil system. In order to develop a uniform, remanent magnetization in each sample, the rock cores were located in the center of the cavity between the coils with the axis of the sample parallel to that of the magnetic field. A DC voltage was applied to the Helmholtz coils sufficient to produce a magnetic field of up to 100 Oe along the axis of the system using a Hewlett Packard 0-24 volt power supply.

In order to insure that the magnetic mineralogy was not oxidized as the samples were heated to 600°C, the oxygen fugacity in the furnace was controlled. For the titanomagnetite composition of the rocks, used in this study the stability field at 600°C requires a fugacity,  $f_{O_2}$ , between  $10^{20}$  and  $10^{23}$ . Tests were carried out using argon to control the fugacity. Argon was streamed into the furnace assembly at a rate of 1.0 l/min at a small positive pressure. (The gas was dried as it flowed through a desiccant prior to entering the furnace.) This technique resulted in an oxygen fugacity of  $10^{20}$  at 600°C.

Since the observed fugacity was on the low end of the stability field, samples were studied after high temperature excursions for signs of oxidation. Specifically, the Rapidan gabbro was examined in detail. Samples were heated to 600°C in the furnace under ambient atmospheric conditions and under a controlled oxygen fugacity and then compared with virgin samples. A visual inspection showed that the samples heated under controlled conditions were indistinguishable from the virgin samples, whereas the samples heated under atmospheric conditions exhibited marked oxidation. Thin sections were prepared from these samples and compared with samples that had not been heated. There were no visible differences. Only the specimen heated under ambient laboratory conditions showed pronounced oxidation throughout the thin section. Based on this observation all samples were heated in an argon environment.

Next, the remanent intensity and orientation of the magnetic moment was measured with an array fluxgate magnetometers in a mu metal shield. Only samples with a magnetic vector within 4° of the sample axis were selected from compressional tests. By varying the field developed by the Helmholtz coils up to 100 Oe remanent intensities up to  $0.058 \text{ emu} \cdot \text{cm}^3$  have been developed in the diabase and  $0.148 \text{ emu} \cdot \text{cm}^3$  have been achieved in the gabbro. The thermoremanent intensity of the diabase is nearly a factor of two lower than that for the gabbro although the TRM was induced

at the same field strength. This is consistent with the fact that the magnetic susceptibility of the gabbro is slightly greater than twice that of the diabase. No attempt has been made to increase the remanent intensities beyond those developed in an inducing field of 100 Oe. The emphasis has been to study only samples that exhibit stable remanent moments; during the next phase of the study the inducing field strength will be increased and the stability of the TRM will be examined as a function of initial intensity.

Cyclic deformation tests were conducted in a 2,000 bar beryllium copper pressure vessel as shown in Figure 7. All the component parts of the pressure vessel were fabricated of beryllium copper hardened to  $R_c = 39$ . Beryllium copper was used because it has a small remanent magnetization ( $10^{-6}$  emu/cm<sup>3</sup>) and a low magnetic susceptibility. The pressure vessel was encased in a two-layer mu-metal shield which attenuated the external field to several hundred gammas. The pressure vessel, encased in the mu-metal shield, was bolted into a hydraulic press fitted with a beryllium copper end plate. The conventional mild steel end plate had to be replaced with a beryllium copper end plate because nonreproducible, viscous remanent magnetic variations *leaked* into the test vessel through the opening in the cap of the mu-metal shield, making reliable magnetic measurements difficult.

A schematic diagram of the sample assembly and flux gate magnetometer sensors is also shown in Figure 7. Beryllium copper spacers were positioned at each end of the sample, and all three pieces were jacketed in 0.13 mm thick copper. The sealed sample was then clamped to the base plug, inserted in the pressure vessel, and a confining pressure of up to 2,000 bars was imposed. A differential stress was applied to the sample by advancing the piston of the hydraulic cylinder driven with an air hydraulic booster. The force on the sample was measured to an accuracy of 1% with an external load cell.

The change in each component of the remanent magnetic vector of the sample was measured with unpotted flux gate magnetometer heads supported with a nylon holder. The magnetometers were Schonstedt DM-2220 digital magnetometers with a resolution of 1 gamma (0.01 mG) over the range of 0-2000 gammas. Two pairs of magnetometers were positioned as shown in Figure 7. One pair measured the axial and radial component of magnetization of the rock sample. The second set of magnetometers was positioned around a beryllium copper cylinder to monitor changes in the axial and radial component of the magnetic field inside the vessel during a loading cycle. The axial magnetometers were positioned as far away from each other as possible so that the magnetometers would not interact and the remanent magnetization of the sample would not bias the background field measurement in the beryllium copper vessel. With the use of these four magnetometers by subtracting the axial and radial magnetometer readings for the rock sample from the axial and radial readings obtained in proximity to the beryllium copper cylinder, the change in remanent magnetization of the rock as a function of stress could be simply obtained.

Cyclic loading experiments were carried out on every sample over one of two possible paths while monitoring the change in remanent magnetization:

1. Cyclically pressurize the specimen to 2,000 bars confining pressure increasing the pressure on each cycle and reducing the pressure to zero at the end of each cycle. Next, hold the confining pressure at 500 bars and cyclically apply a differential stress up to a peak stress of 4,000 bars. Only the differential stress is fully relieved at the termination of each cycle.

2. Apply a confining pressure of 50 bars and then cyclically load the specimen to 2,000 bars differential stress augmenting the stress on each cycle. The differential stress is reduced to zero at the termination of each cycle. Next, the confining pressure is raised to 500 bars and a cyclic load is once again applied, increasing the peak stress on successive cycles up to 4,000 bars. The differential stress is reduced to zero at the termination of each cycle.

These two paths were chosen so that the relative effect of confining pressure and differential stress on changes in TRM could be evaluated. In addition, the magnitude of the piezomagnetic effect on differing rock types would be readily detectable. Since both loading paths terminate at a differential stress of 4,000 bars at 500 bars confining pressure, the role of loading path on permanent demagnetization could be addressed. If the total demagnetization is independent of path, then specimens with identical initial intensities but tested with different stress histories, should exhibit the same post test remanent magnetization.

The results of a typical experiment are presented in Figure 8a and 8b. A gabbro specimen with an initial remanent intensity ( $J_0$ ) of 0.0967 emu cm<sup>3</sup> was cyclically pressurized to 2,000 bars. The magnetization, normalized to its initial value ( $J_0$ ), is plotted as a function of pressure in Figure 8a and a function of differential stress in Figure 8b. The X's indicate the observed magnetization at the peak stress for the cycle and the squares represent the value of the magnetization at the termination of a load cycle due to the peak load for the cycle and plotted at the corresponding pressure. For example, in Figure 8a the sample was pressurized to 2,000 bars in eleven stress cycles. Consider the stress cycle to 1,300 bars. At a pressure of 1,300 bars the sample magnetization was 79 percent of its initial value; upon unloading, it recovered to 81 percent of its initial value. Both data points are plotted at 1300 bars with the X's representing the stressed state and the squares indicating the stress free conditions. At the termination of the hydrostatic pressurization to 2,000 bars, the magnetization of the sample was 76 percent of its preloaded value.

Figure 8b shows the effect of differential stress on remanent magnetization at a confining pressure of 500 bars. The X's represent the magnetization at stress and the squares the value of the magnetization at the termination of the stress cycle. Note that the initial magnetization has already been reduced by 24 percent during the 2,000 bar pressurization. An examination of the test results show that while there is pronounced demagnetization at stress, the recovery upon unloading is greater than that observed during the hydrostatic cycle. For example, at a

differential stress of 2,000 bars the observed magnetization was 0.51 Jo, whereas at the termination of the cycle the value recovered to 0.61 Jo. At the conclusion of the test on gabbro sample 209, a permanent demagnetization of 56 percent or 0.0433 emu/cm<sup>3</sup> was observed.

Figures 8a through 11b show the results of similar experiments on gabbro the initial intensity was successfully increased from 0.097 to 0.131 emu cm<sup>3</sup>. Comparing the results of Figures 8a, 9a and 11a, two facts become obvious: (i) during cyclic pressurization, the peak demagnetization under stress is nearly the same as that recorded at the end of the cycle and (ii) the relative amount of demagnetization due to 2,000 bars of pressure does not dramatically increase with increasing initial TRM.

A similar suite of experiments on the Ralston diabase shows the same effects (Figures 17a, 19a and 20). For the diabase the range of initial intensities is not quite as great as for the gabbro. For each specimen the permanent demagnetization at the termination of a cycle differed only slightly from the demagnetization observed at stress.

If hydrostatic pressurization to 2,000 bars can reduce the remanent intensity by 20 - 30 percent, what is the effect at 2,000 bars of differential stress? A comparison of the results in Figures 8a and 15 for gabbro and Figures 18a and 21a for diabase shows the typical behavior observed for these rocks. First, for nearly identical initial intensities on the same rock type a differential stress of 2,000 bars produces more permanent demagnetization than hydrostatic pressure to the same level. For the gabbro, the 2,000 bars of uniaxial compression permanently demagnetized gabbro 211, 37 percent (Figure 15) while hydrostatic pressure resulted in a permanent decrease of only 24 percent on gabbro 209 (Figure 8a). Similarly for the Ralston diabase, a differential stress of 2,000 bars produced a 65 percent decrease in the remanent moment (Figure 21a) whereas the application of 2,000 bars of pressure resulted in a permanent change of 45 percent (Figure 18a). Furthermore, during the unload portion of a differential stress cycle the magnetic recover is appreciably greater than for the hydrostatic case.

The hydrostatic cyclic and differential stress cyclic loading tests to 2,000 bars demonstrates that for identical specimens with the same initial magnetization, differential stress produces greater demagnetization than hydrostatic pressurization. This is certainly apparent when the greatest principal stress direction is coincident with the remanent vector. For other orientations of the TRM the difference may not be as pronounced.

The effect of initial remanent intensity on the piezomagnetic effect is graphically shown for the gabbro in Figure 17. The change in remanent magnetization (at the conclusion of a stress cycle) is plotted as a function of the peak differential stress on each cycle for three initial intensities, 0.0339, 0.0629 and 0.1480 emu/cm<sup>3</sup>. The magnetization presented in Figure 17 is the axial component of the magnetic vector, in millgauss, as observed in the pressure vessel. Since no change in the radial component of the magnetic vector was observed, the change in the axial component is directly proportional to the change in the TRM. The data shows that with increasing initial intensity, the permanent demagnetization per increment of stress increases. Furthermore the piezomagnetic sensitivity is greatest at low stresses.

Finally, the effect of path on the total piezomagnetic effect must be addressed. Two experiments on Ralston diabase 01 and 02 are well suited for comparison. The initial intensities are similar 0.0358 (Ralston 01) and 0.0310 (Ralston 02); Ralston 01 was cyclically pressurized to 2,000 bars (Figure 18a) and then loaded to a differential stress of 4,000 bars (Figure 18b) whereas Ralston 02 was uniaxially loaded to 2,000 bars (Figure 21a) and then compressed to 4,000 bars at a confining pressure of 500 bars Figure 21b). First, compare the results in Figures 18b and 21b. at the end of the 4,000 bar stress cycle, the total demagnetization is very close to the same. Ralston 01 demagnetized to 18 percent of its initial value and Ralston 02 to 19 percent of its pre-stressed value. Both have arrived at nearly the same final magnetization but over much different paths. An examination of Figures 18a and 21a shows that initial pressurization to 2,000 bars resulted in a 45 percent reduction in

magnetization while differentially loading the sample to 2,000 bars produced a larger change of 65 percent. Consequently, the stress sensitivity during the 4,000 bar differential stress loading sequence was appreciably greater for Ralston 01 than for Ralston 02. Further examination of Figure 18b and 21b also suggests that at stresses above 2,000 bars both specimens exhibit the same stress sensitivity; that is the change in rock magnetization per incremental increase in stress.

#### CONCLUSIONS AND PRECOMMENDATIONS

From the data collected over the first year of this study several important characteristics of piezomagnetism have been observed. First, non-hydrostatic stress exhibits a greater stress sensitivity than simple pressurization. Second, the magnitude of the piezomagnetic effect increases with increasing TRM. The change in magnetization with increasing stress is not linear; it is larger at low stresses and diminishes with increasing stress. Third, the total permanent demagnetization appears to be independent of path at least for the situation where the final segment involves loading to a differential stress greater than the peak mean stress experienced during previous cycles.

*Pike et al. (1981)* studied the effect of differential stress and pressure on the remanent magnetization of several rock types. While the study was not exhaustive, they noted that the rate of change of magnetization with increasing differential stress was substantially the same during that observed during pressurization. Obviously, their results conflict with what we have observed. Several reasons for this dichotomous behavior exist. First, in this study the remanent vector for every sample was coincident with the axis of the specimen and the loading direction in the non-hydrostatic loading segments. This orientation maximizes the piezomagnetic change due to non-hydrostatic testing. When the remanent vector is inclined to the greatest principal stress direction, the situation may not be as simple. For the limiting case in this study, only the magnitude of the magnetic vector changed but the orientation remained constant. However, when the remanent vector is inclined to the greatest principal stress direction, the orientation as well as the magnitude of the remanence changes. It is entirely possible that for a

range of orientations, the magnitude of the piezomagnetic effect is similar for both loading conditions. Alternatively, there may be fundamental differences in the behavior of titanomagnetite crystals of different grain size and composition. In order to resolve this difficulty, samples of the rocks reported on by *Pike et al. (1981)* have been requested, and will be studied.

The fact that increasing the initial magnetic intensity increases the magnitude and stress sensitivity of the piezomagnetic effect is very encouraging. Coupled with the observation that the greatest range of change occurs at low stresses, the results extend the potential range of any piezomagnetic sensor downward from 500 bars to detectable changes on the order of 100 bars. The only potential drawback to using specimens with large initial magnetizations is the stability. Ideally it would be advantageous to increase the magnetization of a sample to saturation while maintaining hard remanence. Unfortunately, this is not possible. During the next year of this study of the stability of the TRM will be examined as a function of the magnitude of the remanent moment.

For the two loading paths that have been reported here, the total piezomagnetic change appears to be independent of path. This observation is far from being universally demonstrated. Given the fact that the change due to pressure is substantially less than that observed at a differential stress of the same value, it appears that *path independence* may only occur when differential loading constitutes the final loading segment. Furthermore, the differential stress during the final loading segment must exceed the mean at peak stress that the sample has been subjected to previously. Future experiments will be designed to develop this point in more detail.

During the second year of this contract, the points outlined above for further study will be addressed. In addition, a detailed examination of the microstructure of the magnetic grains will be carried out using a scanning electron microscope (SEM). Differences in the piezomagnetism of varying titanomagnetite compositions and grain size will be evaluated in terms of the SEM results.

## REFERENCES

Boyd, J. R., M. Fuller and S. Halgedahl, Domain wall nucleation as a controlling factor in the behavior of fine magnetic particles in rocks, *Geophys. Res. Letters*, *11* (3), pp. 193-196, 1984.

Day, R., TRM and its variation with grain size, *Origin of Thermoremanent magnetization*, Center for Academic Publication, Japan, 1977.

Dunlop, D.J., Thermoremanent magnetization in submicroscopic magnetite, *J. Geophys. Res.* *78*, 1780, 1973.

Halgedahl, S., and M. Fuller, The dependence of magnetic domain structure upon magnetization state with emphasis upon nucleation as a mechanism for pseudo-single domain behavior, *J. Geophys. Res.* *88* (B6), 6505-6522, 1983.

Jelenska, M., Stress dependence on the magnetization and magnetic properties of igneous rocks, *Pure Appl. Geophys.*, *113*, 635-649, 1975.

Kean, W. R., R. Day, M. Fuller and V. A. Schmidt, The effect of uniaxial compression on the initial susceptibility of rocks as a function of grain size and composition of their constituent titanomagnetites, *J. Geophys. Res.*, *81*, 861-872, 1976.

Martin, R. J., III, and M. Wyss, Magnetism of rocks and volumetric strain in uniaxial failure tests, *Pure Appl. Geophys.*, *113*, 169-182, 1975.

Martin R. J., III, R. E. Haberman, and M. Wyss, The effect of stress cycling and inelastic volumetric strain on remanent magnetization, *J. Geophys. Res.* *83*, (B7), 3485-3496, 1978.

Martin, R. J., III, Is piezomagnetism influenced by microcracks during cyclic loading? *J. Geomag. Geoelectr.*, *32*, 741-755, 1980.

Martin, R.J. and J.S. Noel, Peak stress measurements on ONE TON and MINI JADE, DNA report in review, 1984.

Nagata, T., Tectonomagnetism. *Bull. Int. Assoc. Geomagn. Aeron.* 27, 12-43, 1969.

Nagata, T., and B. J. Carleton, Notes of Piezo-remanent magnetization of igneous rocks, III, *J. Geomagn. Geoelect.*, 21, 623-645, 1969.

Ohnaka, M., Stability of remanent magnetization of rocks under compression - its relation to grain size of rock forming ferromagnetic minerals, *J. Geomagn. Geoelect.*, 21, 495-505, 1969.

Ohnaka, M., and J. Kinoshita, Effects of uniaxial compression on remanent magnetization, *J. Geomagn. Geoelect.*, 20, 93-99, 1968.

Pike, S.J., Henyey, T.L., Revol J. and M. D. Fuller, High pressure apparatus for use with a cryogenic magnetometer, *J. Geomag. Geoelectr.*, 33 pp. 449-466, 1981.

TABLE I

## Magnetic Properties

Rock Type	Susceptibility emu/ g - Oe $\times 10^{-3}$	Coercivity Oe	Curie Temp. $^{\circ}\text{C}$	Saturation Magnetization emu/g	Grain Size Microns
Basalt Dotzero, CO	1.73	183.5	570	3.92	1-20
Diabase Golden, CO	2.06		535	2.90	5-100
Gabbro Rapidan, VA	4.85	47.5	580	2.36	5-100
Andesite Mt. St. Helens, WA	1.30	181	560	0.72	1-20
Granite Westerly, RI	1.22	42	580	0.64	1-50

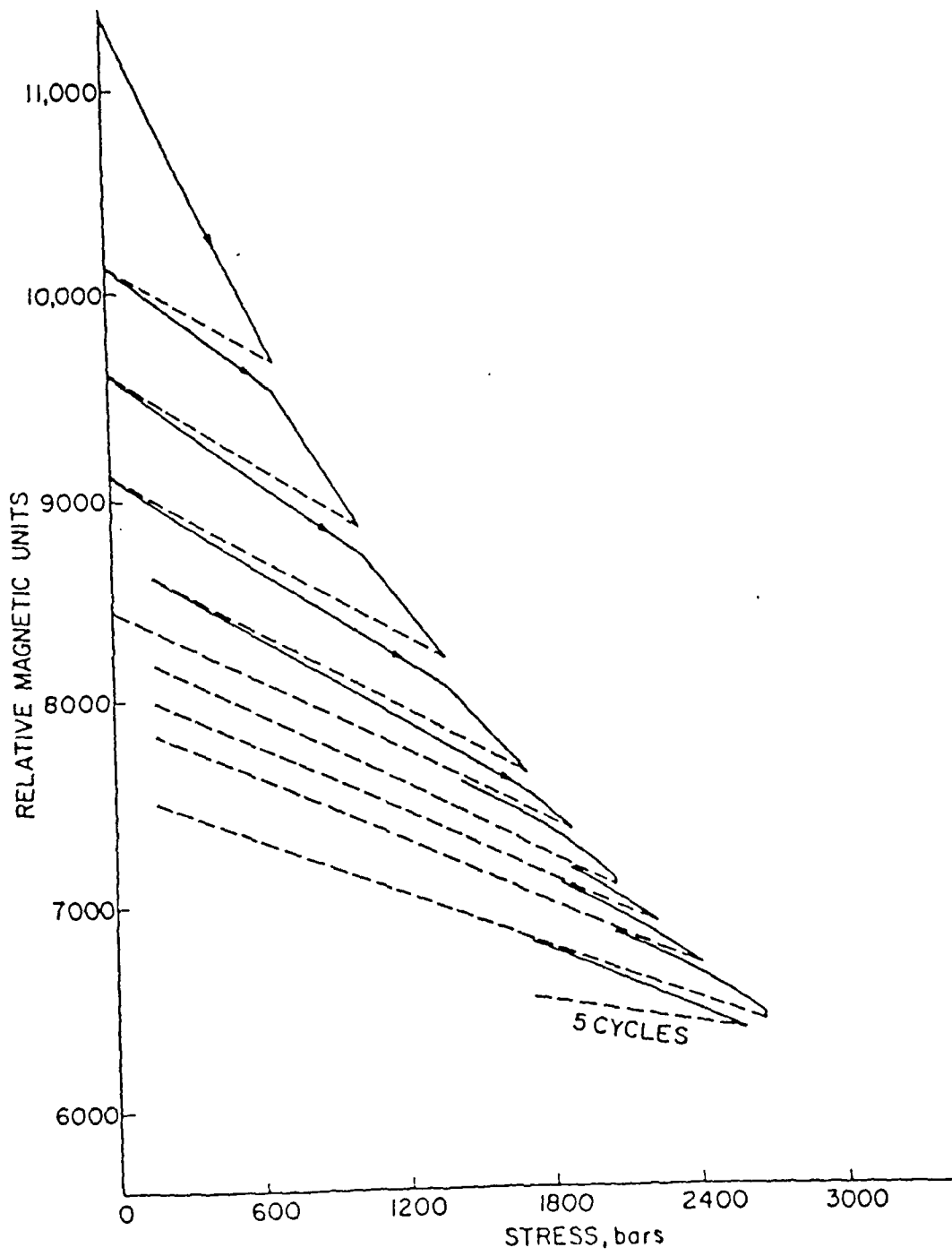


Figure 1. Change in remanent magnetic intensity as a function of stress for a sample loaded in uniaxial compression.

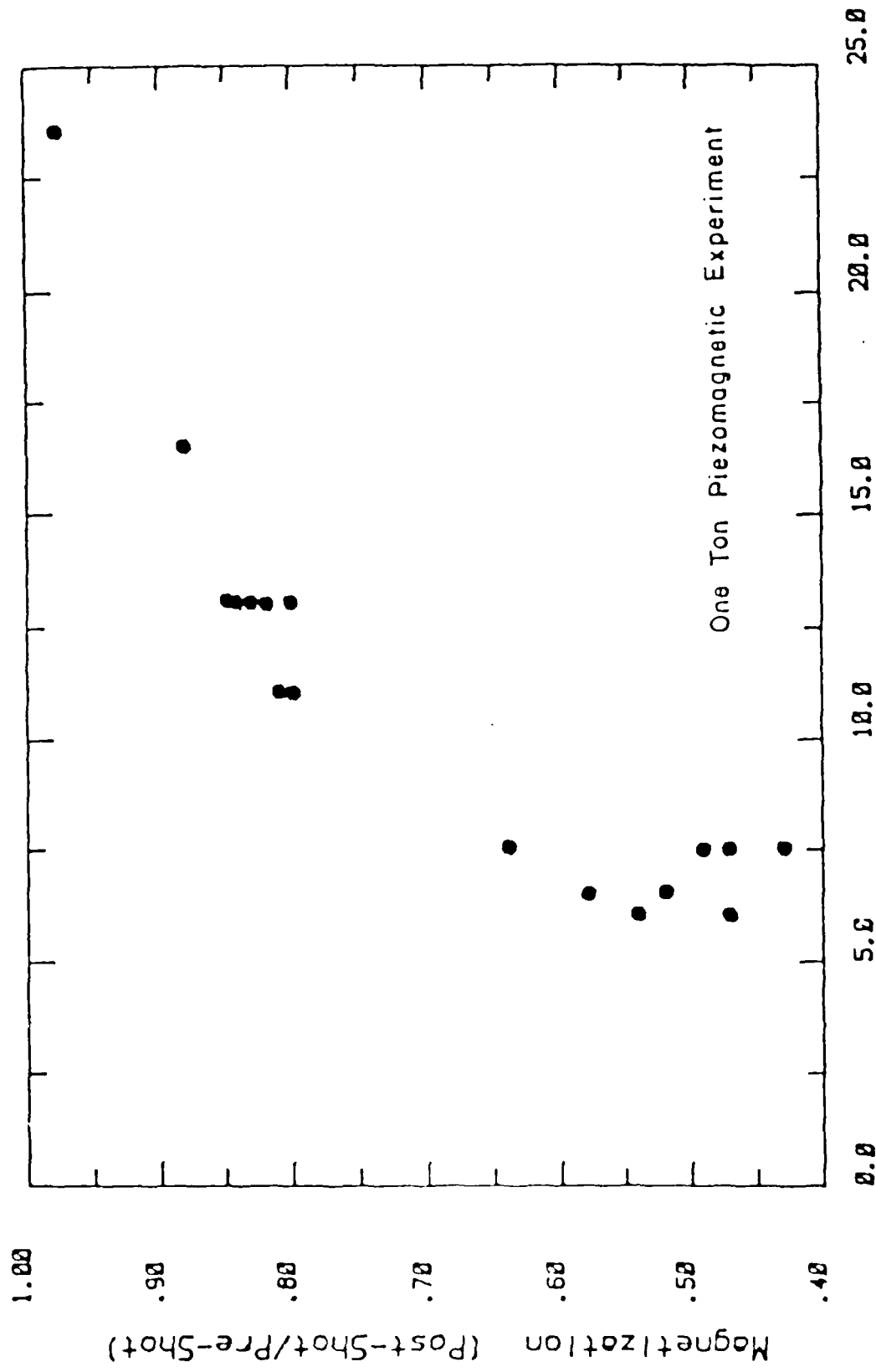


Figure 2. Change in magnetization of the gabbro samples fielded on ONE TON. The ratio of post-shot to pre-shot remanent magnetization is plotted as a function of distance from the working point.

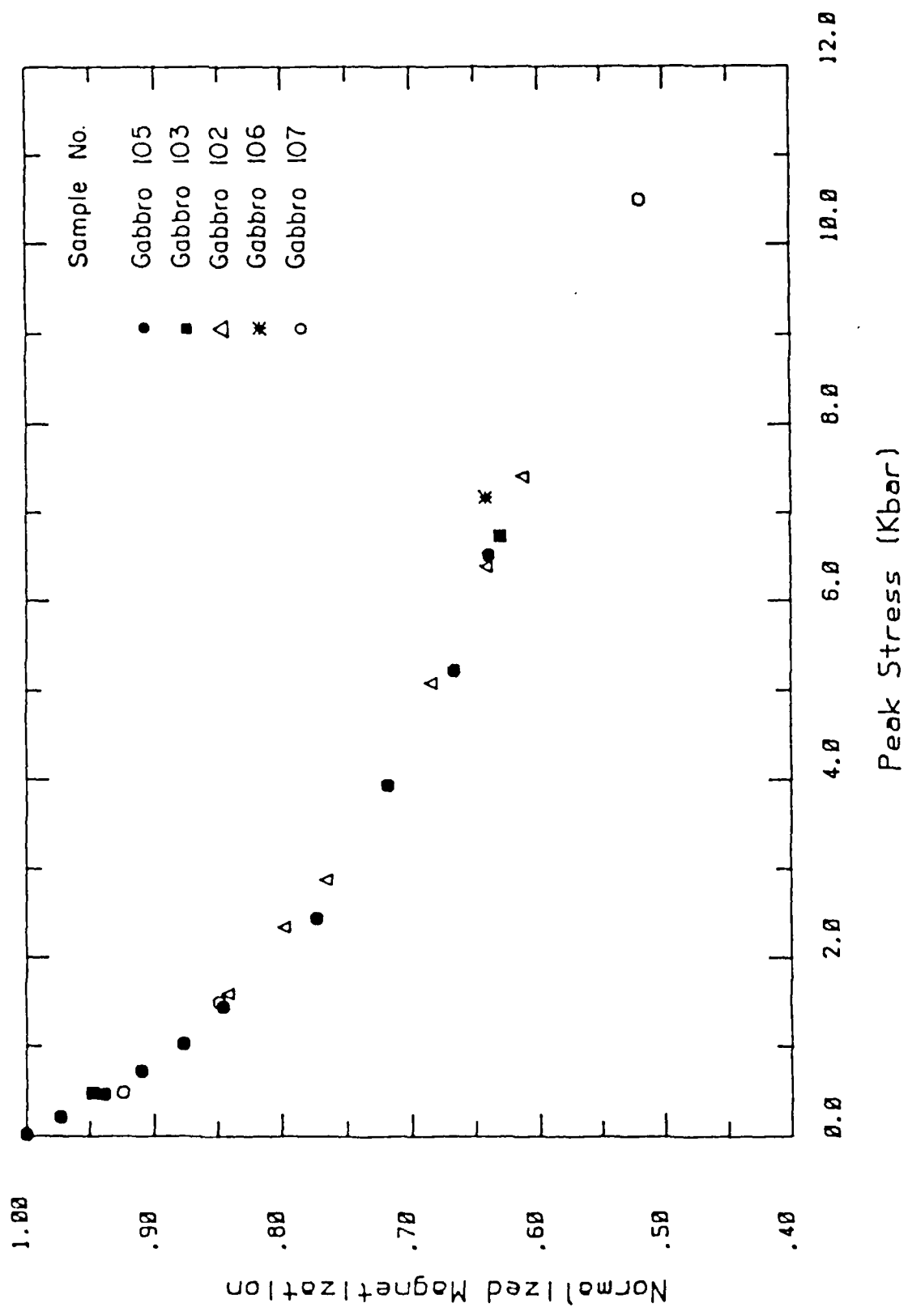


Figure 3. The normalized magnetization for a number of gabbro samples at the termination of a stress cycle is plotted as a function of the peak stress that the sample experienced.

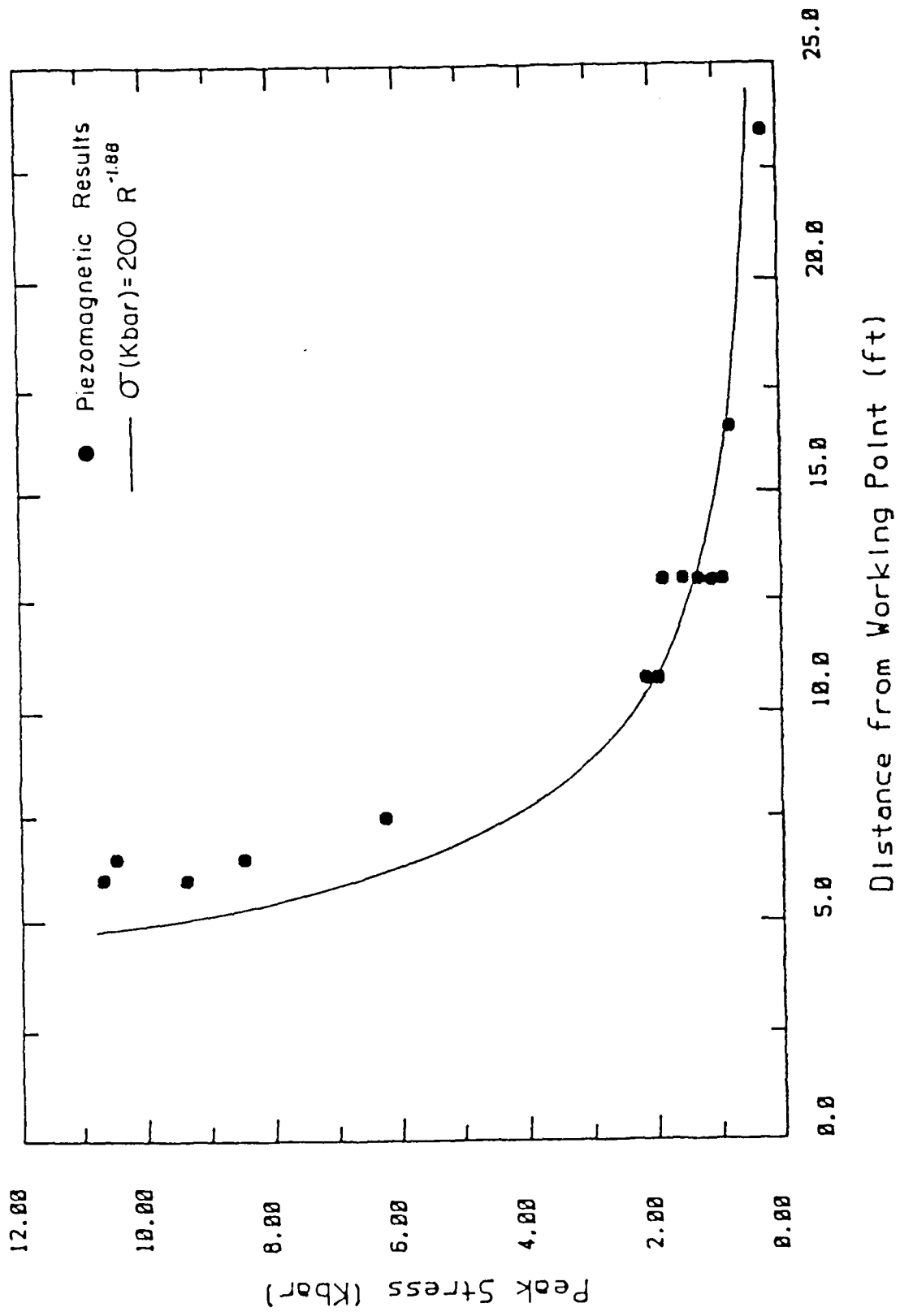


Figure 4. Peak stress as a function of range inferred from the gabbro piezomagnetic rock cores fielded on ONE TON. The solid line is the stress attenuation curve used by Sandia National Laboratories for a one ton yield.

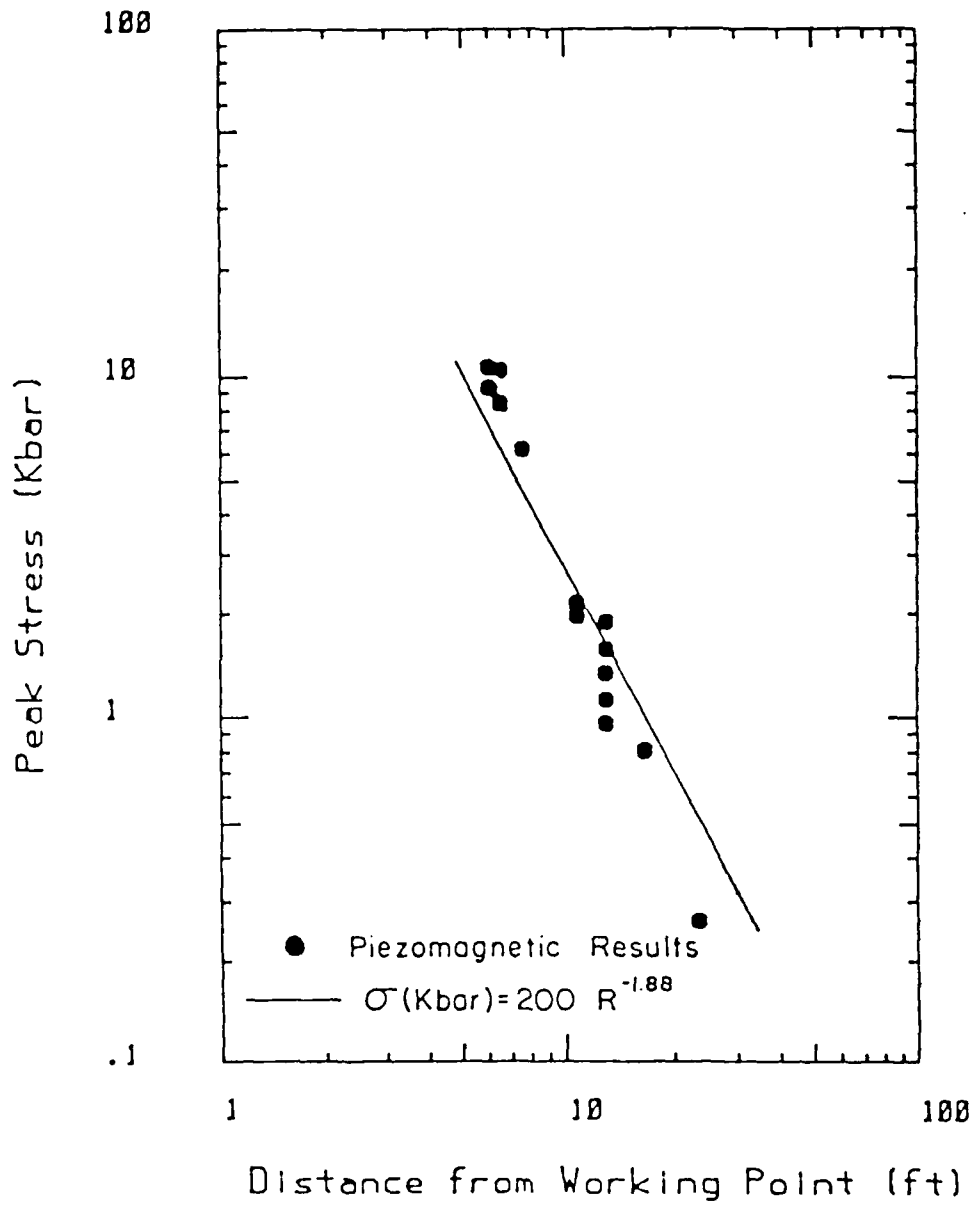


Figure 5. Peak stress as a function of range inferred from the gabbro piezomagnetic rock cores field on ONE TON. The solid line is stress attenuation curve used by Sandia National Laboratories for a one ton yield.

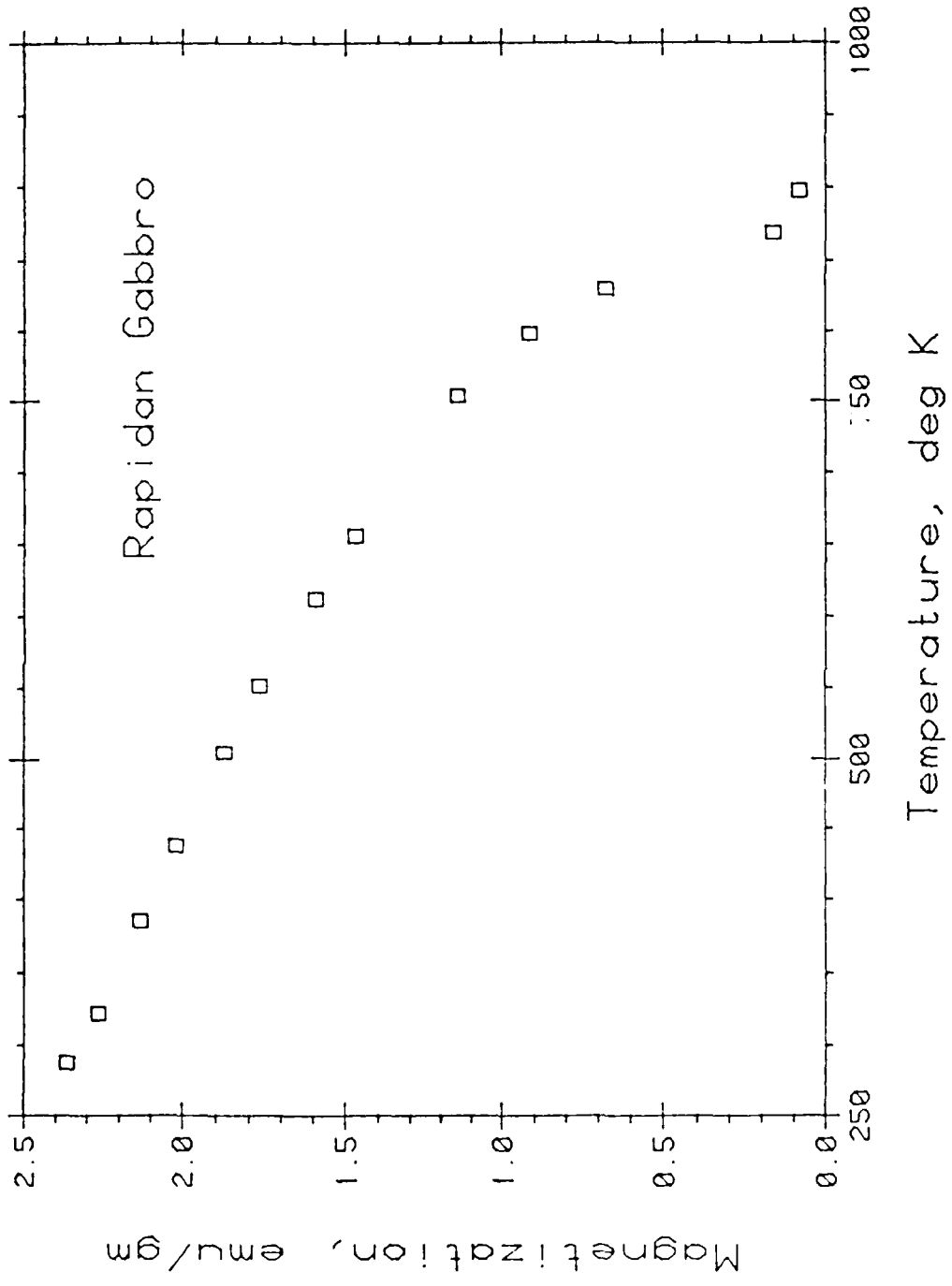


Figure 6. Change in magnetization with increasing temperature for the Rapidan gabbro. At 850°K the magnetization drops to nearly zero. This temperature is taken as the Curie temperature.

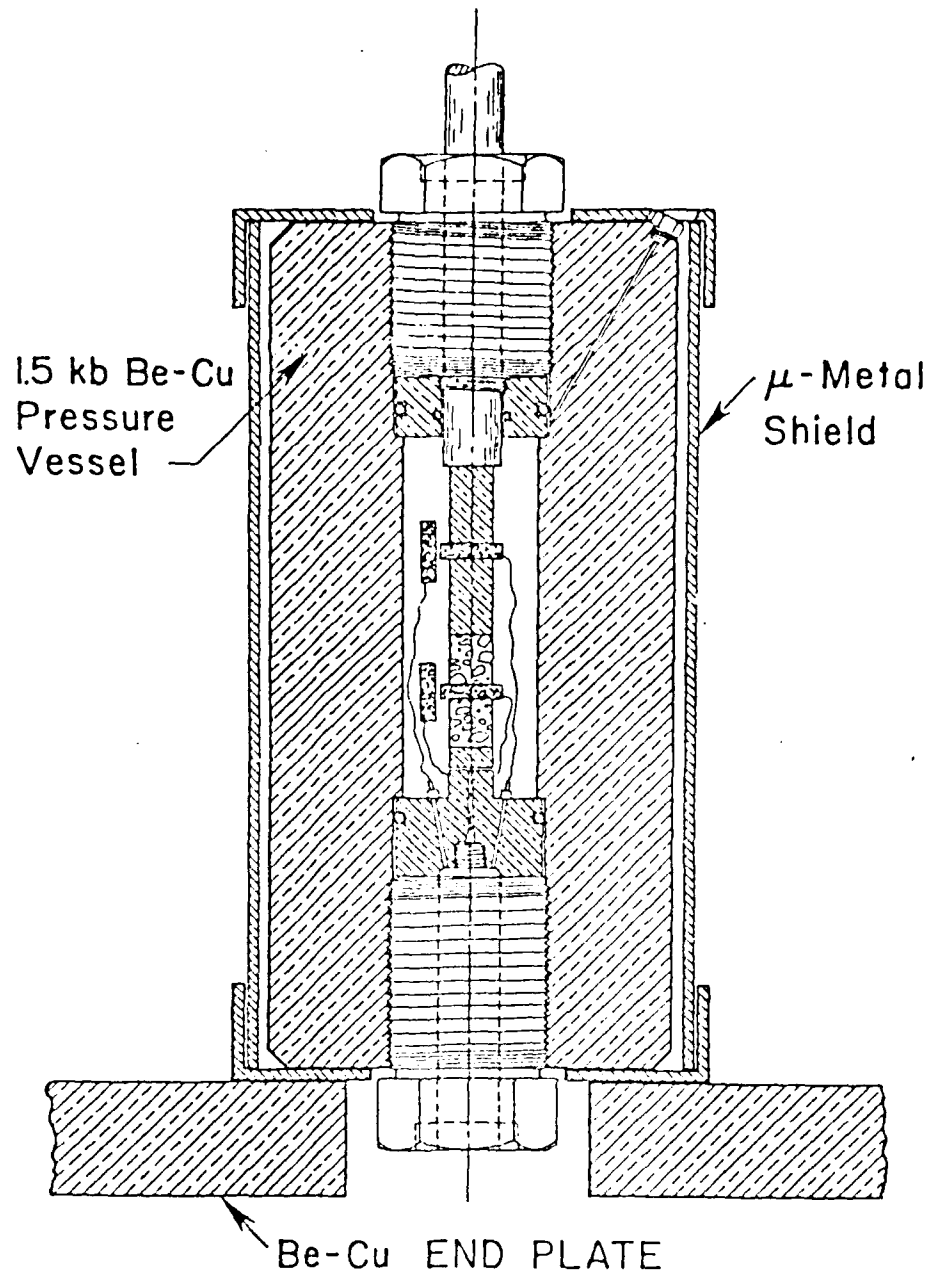


Figure 7. Scale drawing of 2,000 bar beryllium copper pressure vessel, base plug, sample configuration, and flux gate magnetometer array. One pair of magnetometer is positioned around a beryllium copper dummy sample and monitors changes in the background field within the pressure vessel.

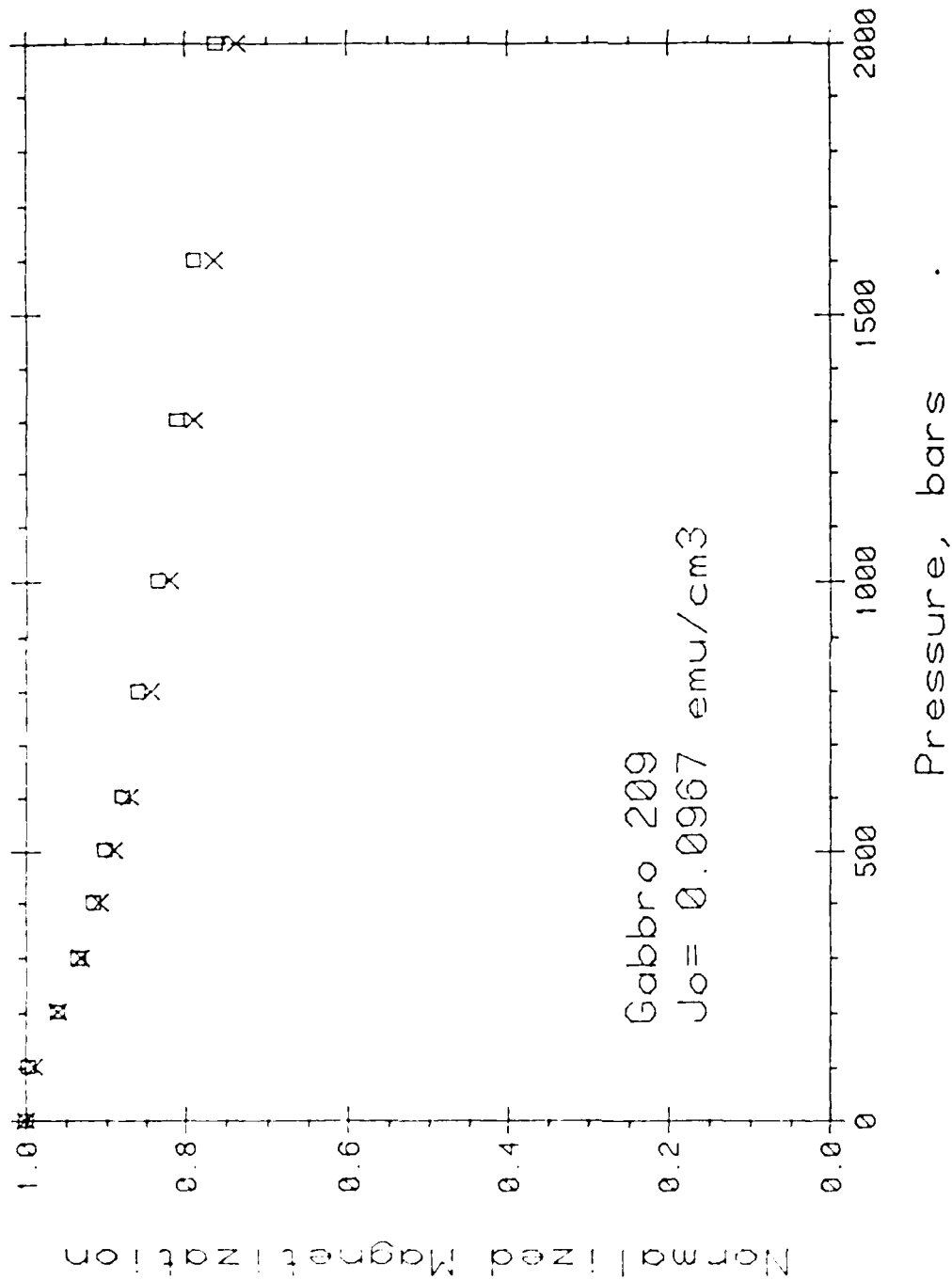
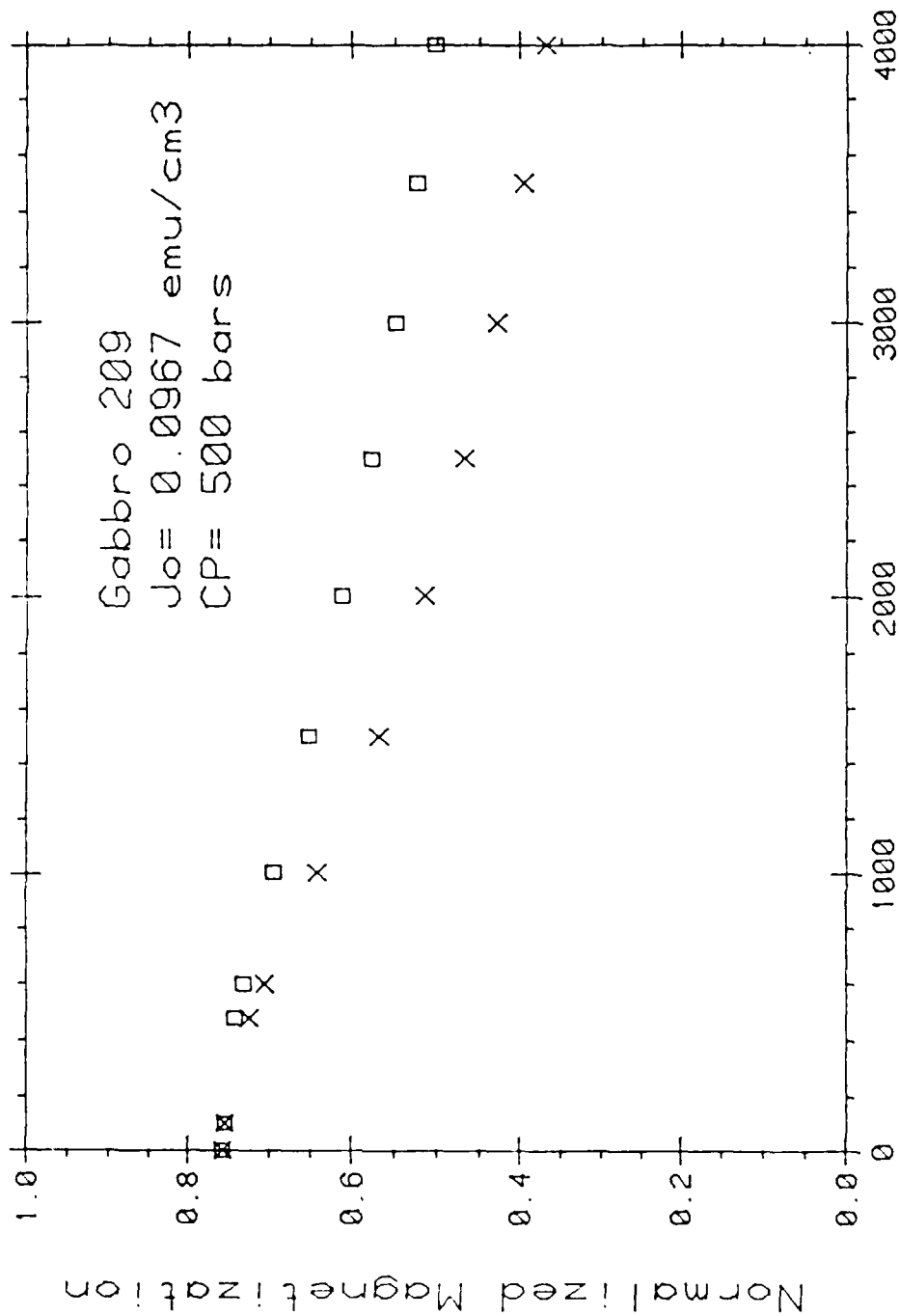


Figure 8a. The change in remanent magnetization, normalized to its initial intensity ( $J_0$ ) is plotted as a function of confining pressure for a cyclic compression test. The X's represent the observed magnetization at the pressure indicated. The squares represent the magnetization at zero pressure, at the end of the cycle; the data point is plotted at the corresponding pressure.



Differential Stress, bars

Figure 8b. The change in remanent magnetization, normalized to its initial intensity ( $J_0$ ), is plotted as a function of differential stress at a confining pressure of 500 bars, for cyclic loading. Only the differential stress was reduced to zero at the termination of each cycle. The X's represent the magnetization of the stress indicated. The squares represent the magnetization at zero stress, at the end of the cycle; the data point is plotted at the corresponding peak stress.

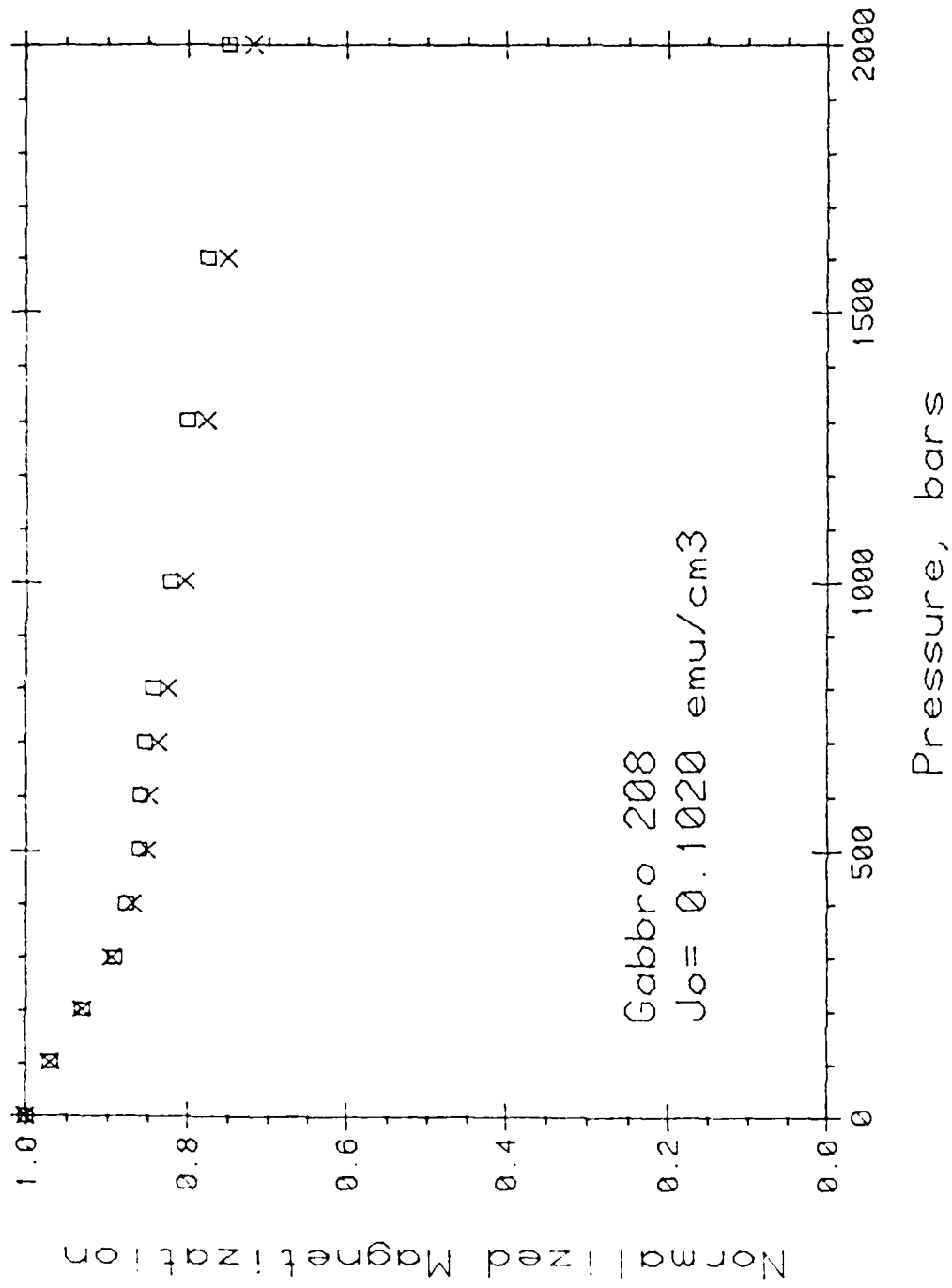


Figure 9a. The change in remanent magnetization, normalized to its initial intensity ( $J_0$ ) is plotted as a function of confining pressure for a cyclic compression test. The X's represent the observed magnetization at the pressure indicated. The squares represent the magnetization at zero pressure, at the end of the cycle; the data point is plotted at the corresponding pressure.

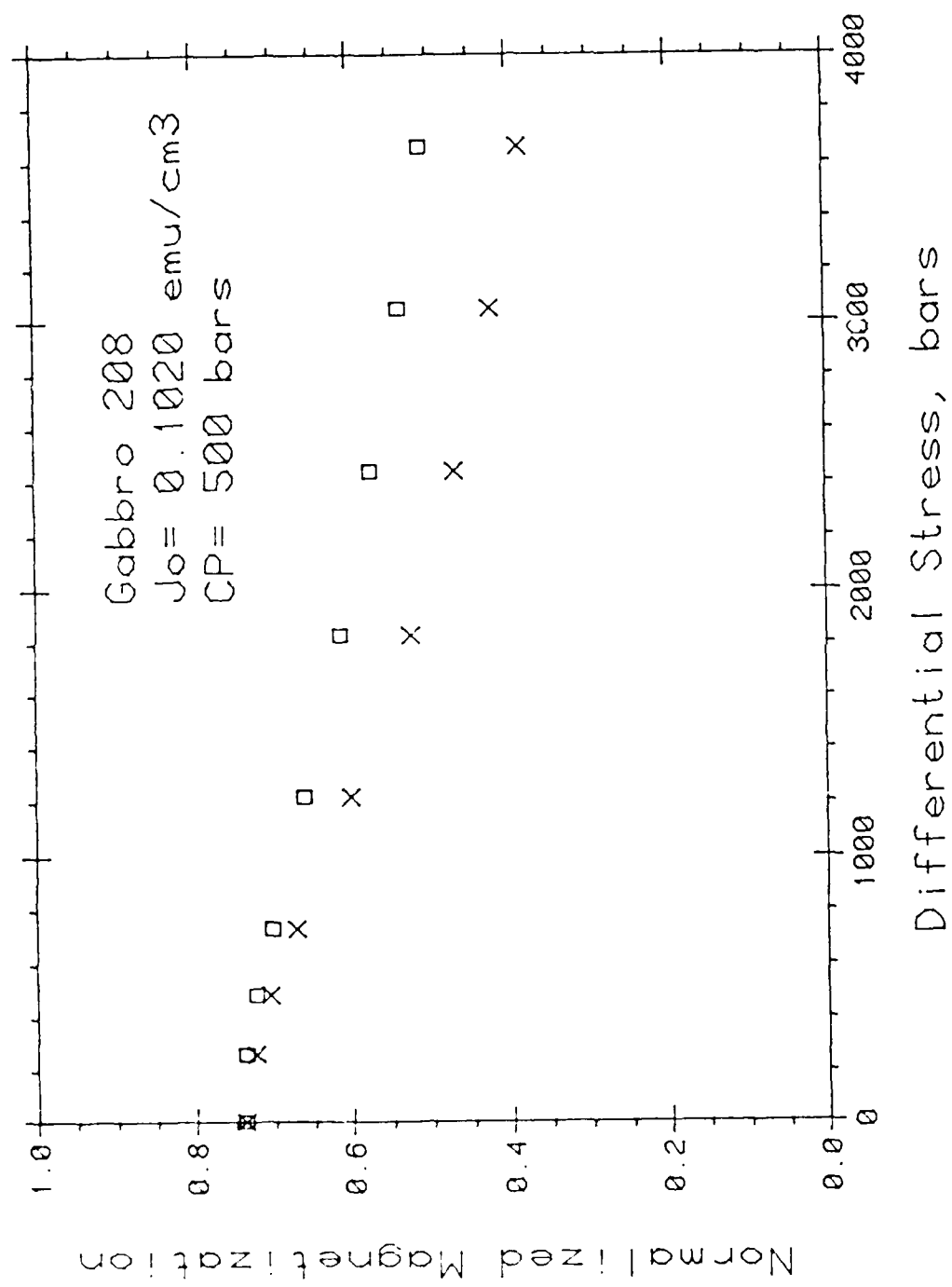


Figure 9b. The change in remanent magnetization, normalized to its initial intensity ( $J_0$ ), is plotted as a function of differential stress at a confining pressure of 500 bars, for cyclic loading. Only the differential stress was reduced to zero at the termination of each cycle. The X's represent the magnetization of the stress indicated. The squares represent the magnetization at zero stress, at the end of the cycle; the data point is plotted at the corresponding peak stress.

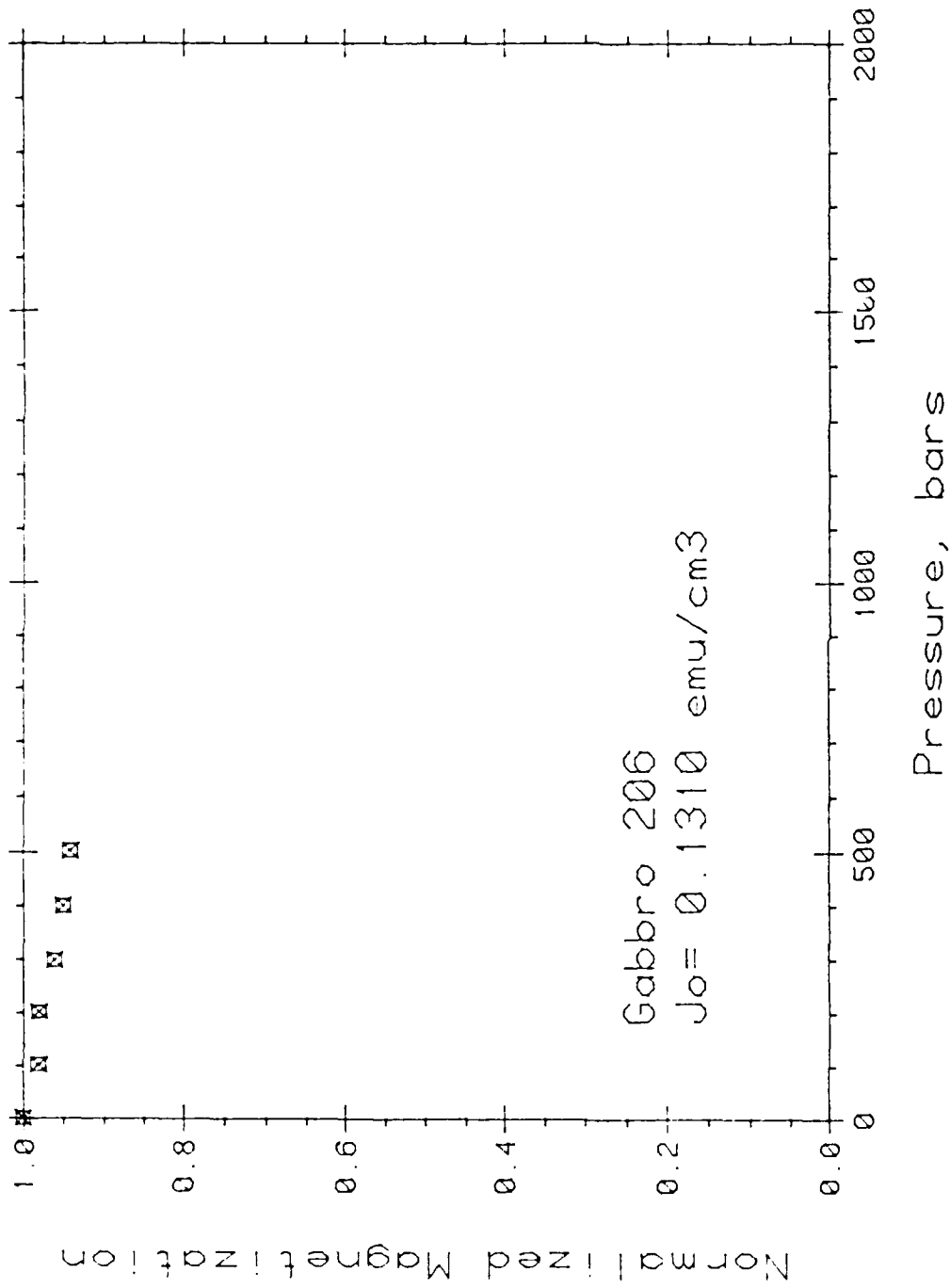


Figure 10a. The change in remanent magnetization, normalized to its initial intensity ( $J_0$ ) is plotted as a function of confining pressure for a cyclic compression test. The N's represent the observed magnetization at the pressure indicated. The squares represent the magnetization at zero pressure, at the end of the cycle; the data point is plotted at the corresponding pressure.

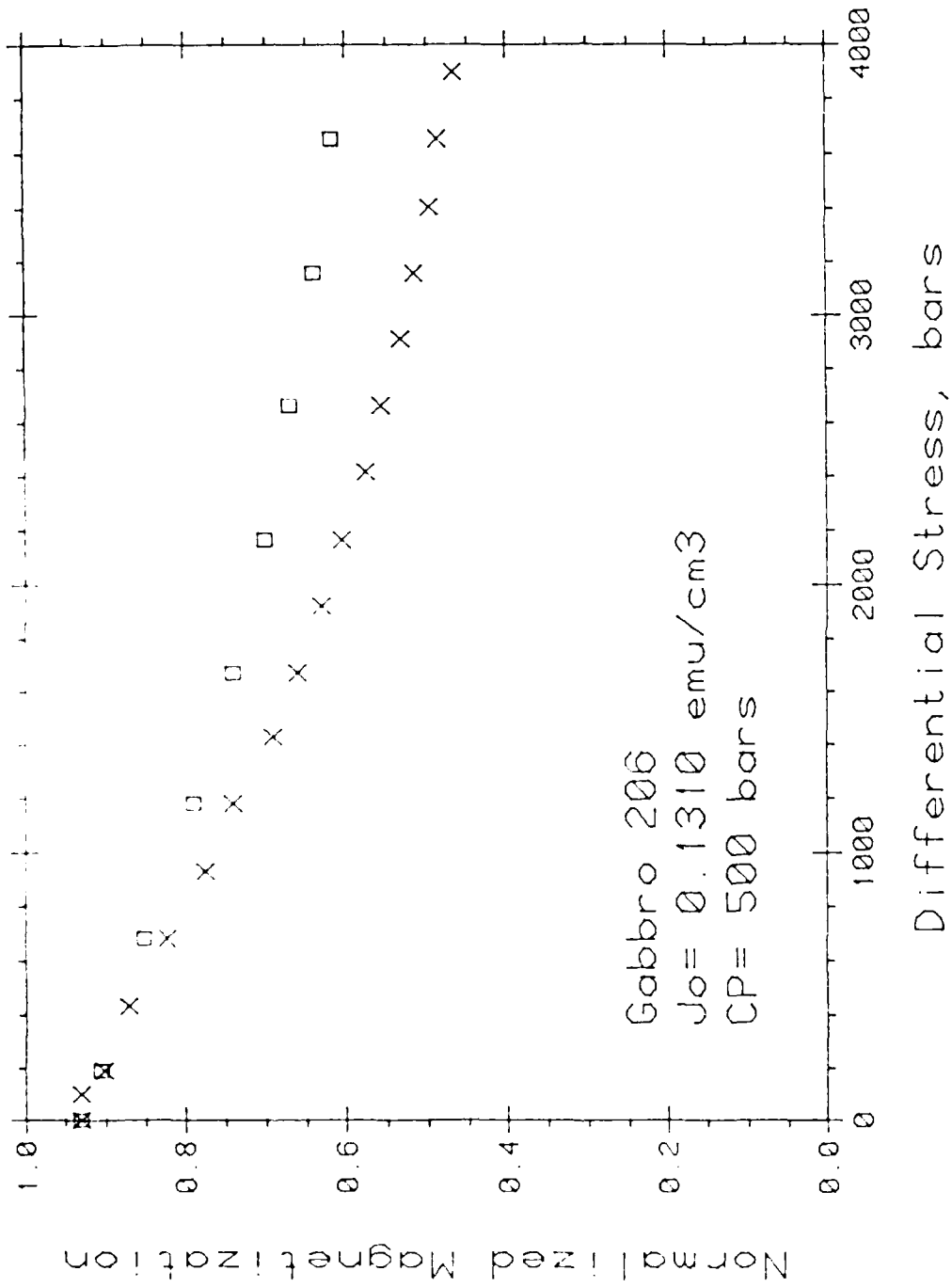


Figure 10b. The change in remanent magnetization, normalized to its initial intensity ( $J_0$ ), is plotted as a function of differential stress at a confining pressure of 500 bars, for cyclic loading. Only the differential stress was reduced to zero at the termination of each cycle. The X's represent the magnetization of the stress indicated. The squares represent the magnetization at zero stress, at the end of the cycle; the data point is plotted at the corresponding peak stress.

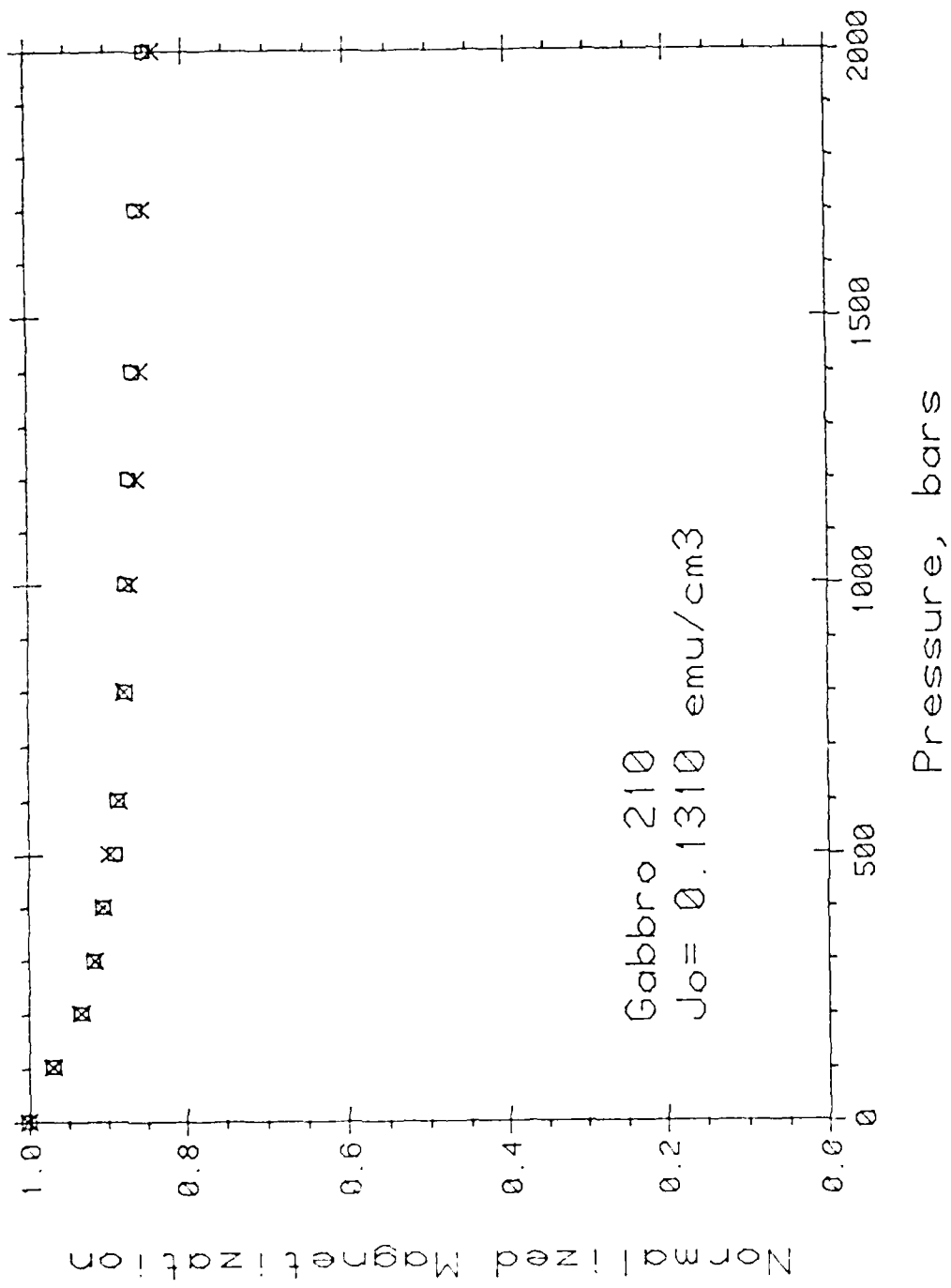


Figure 11a. The change in remanent magnetization, normalized to its initial intensity ( $J_0$ ) is plotted as a function of confining pressure for a cyclic compression test. The X's represent the observed magnetization at the pressure indicated. The squares represent the magnetization at zero pressure, at the end of the cycle; the data point is plotted at the corresponding pressure.

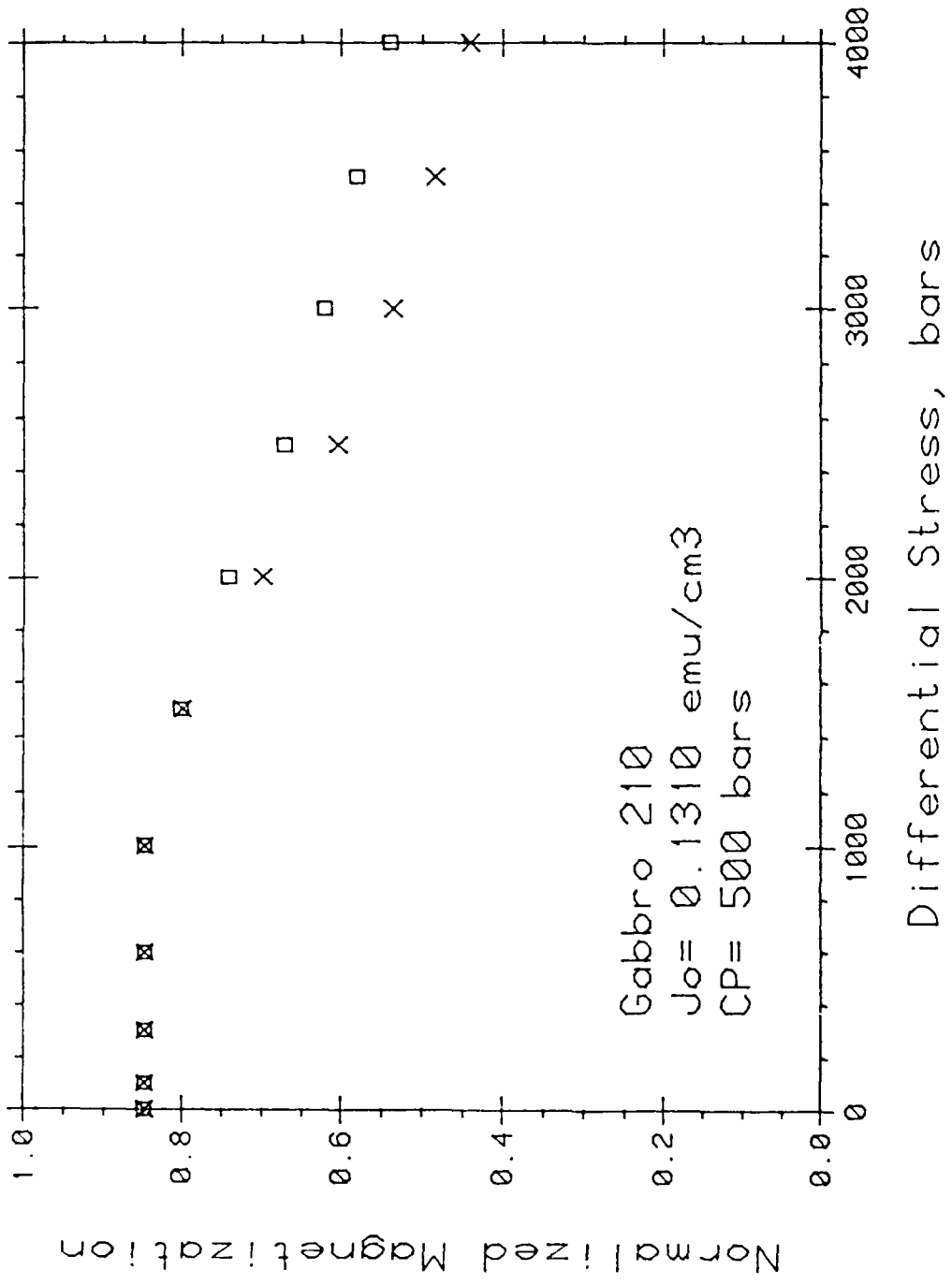


Figure 11b. The change in remanent magnetization, normalized to its initial intensity ( $J_0$ ), is plotted as a function of differential stress at a confining pressure of 500 bars, for cyclic loading. Only the differential stress was reduced to zero at the termination of each cycle. The X's represent the magnetization of the stress indicated. The squares represent the magnetization at zero stress, at the end of the cycle; the data point is plotted at the corresponding peak stress.

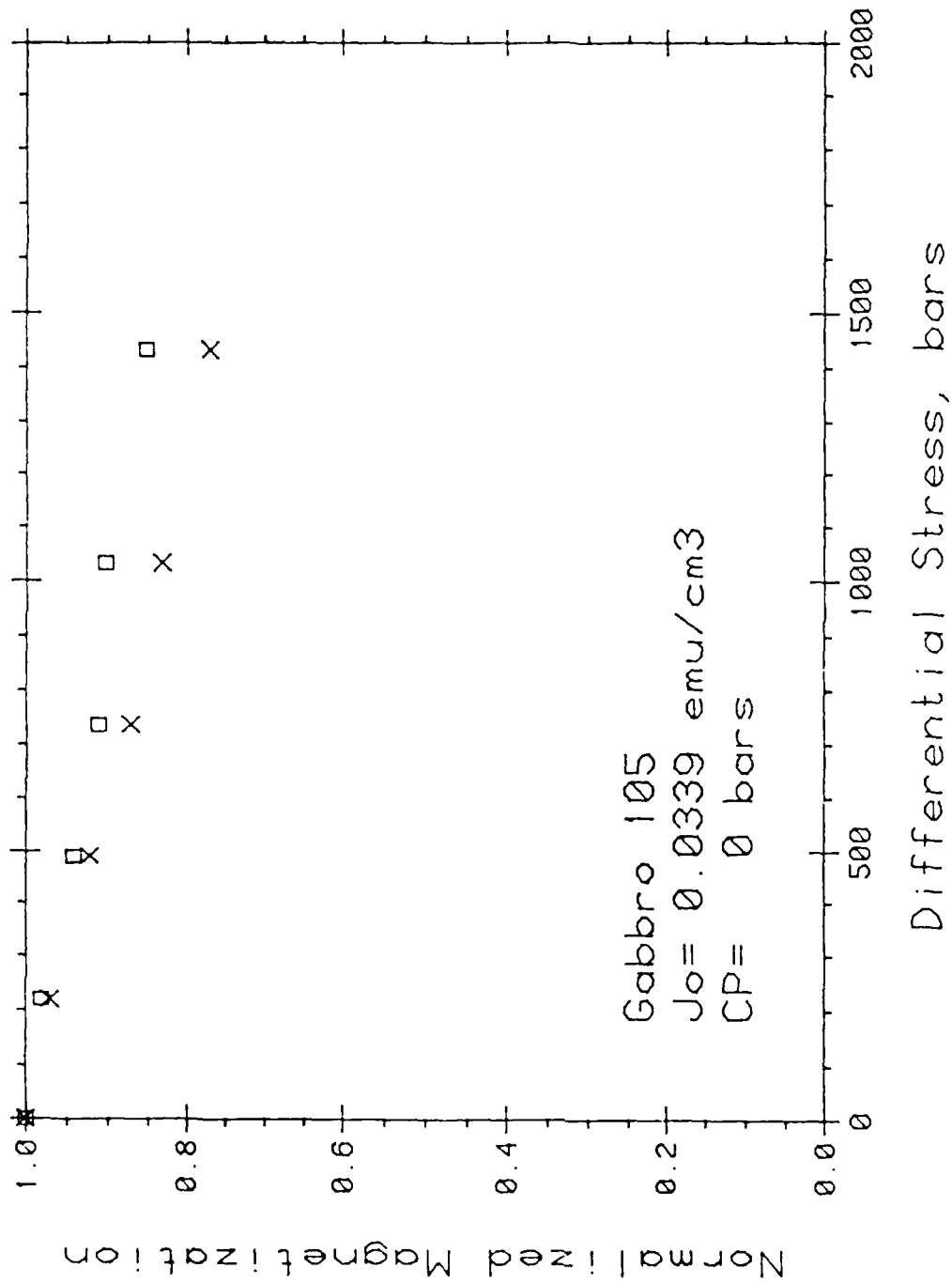


Figure 13. The change in remanent magnetization, normalized to its initial intensity ( $J_0$ ) is plotted as a function of differential stress for a cyclic compression test. The X's represent the observed magnetization at the stress indicated. The squares represent the magnetization at zero differential stress, at the end of the cycle; the data point is plotted at the corresponding differential stress.

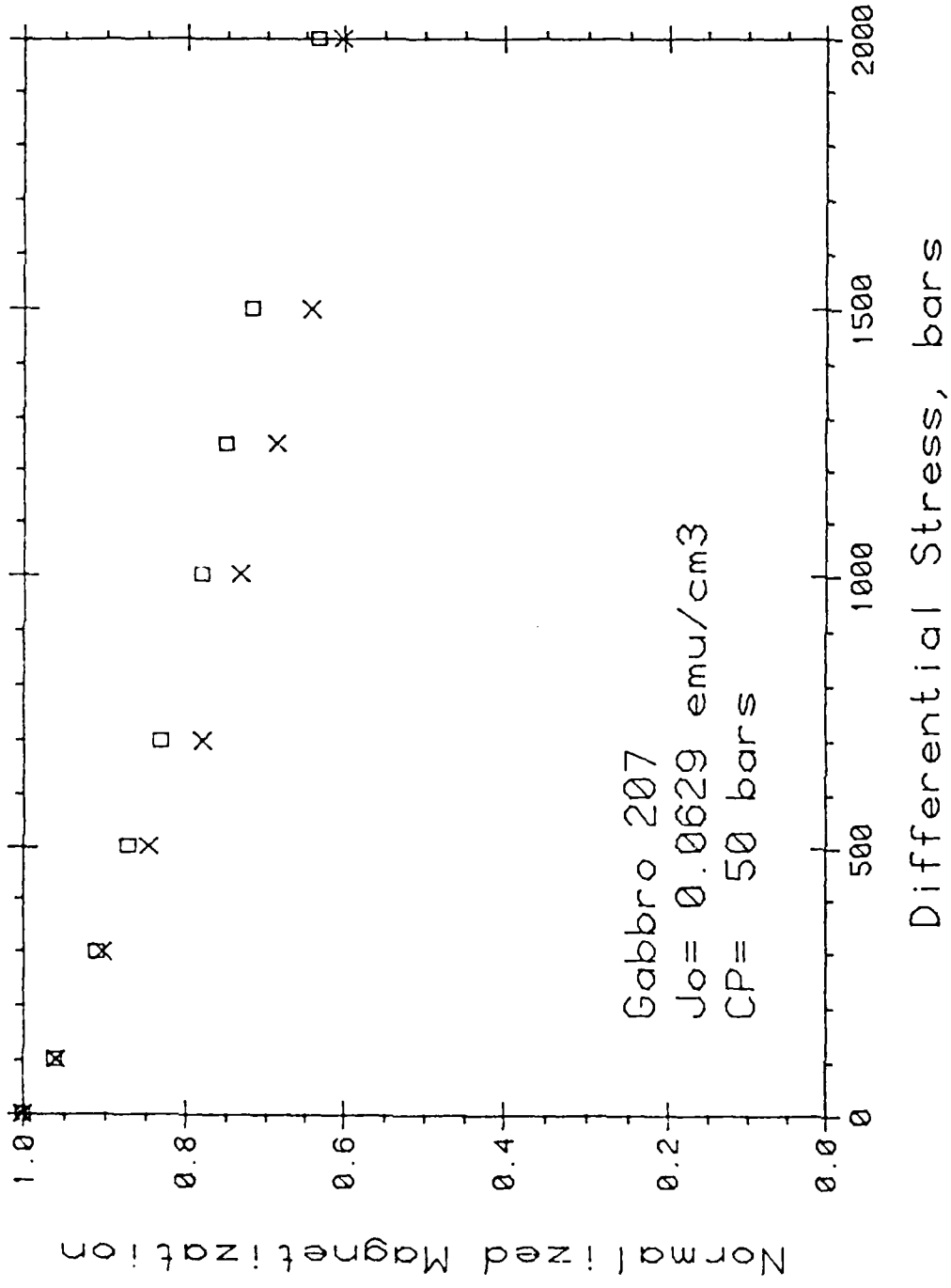


Figure 14. The change in remanent magnetization, normalized to its initial intensity ( $J_0$ ) is plotted as a function of differential stress for a cyclic compression test. The X's represent the observed magnetization at the stress indicated. The squares represent the magnetization at zero differential stress, at the end of the cycle; the data point is plotted at the corresponding differential stress.

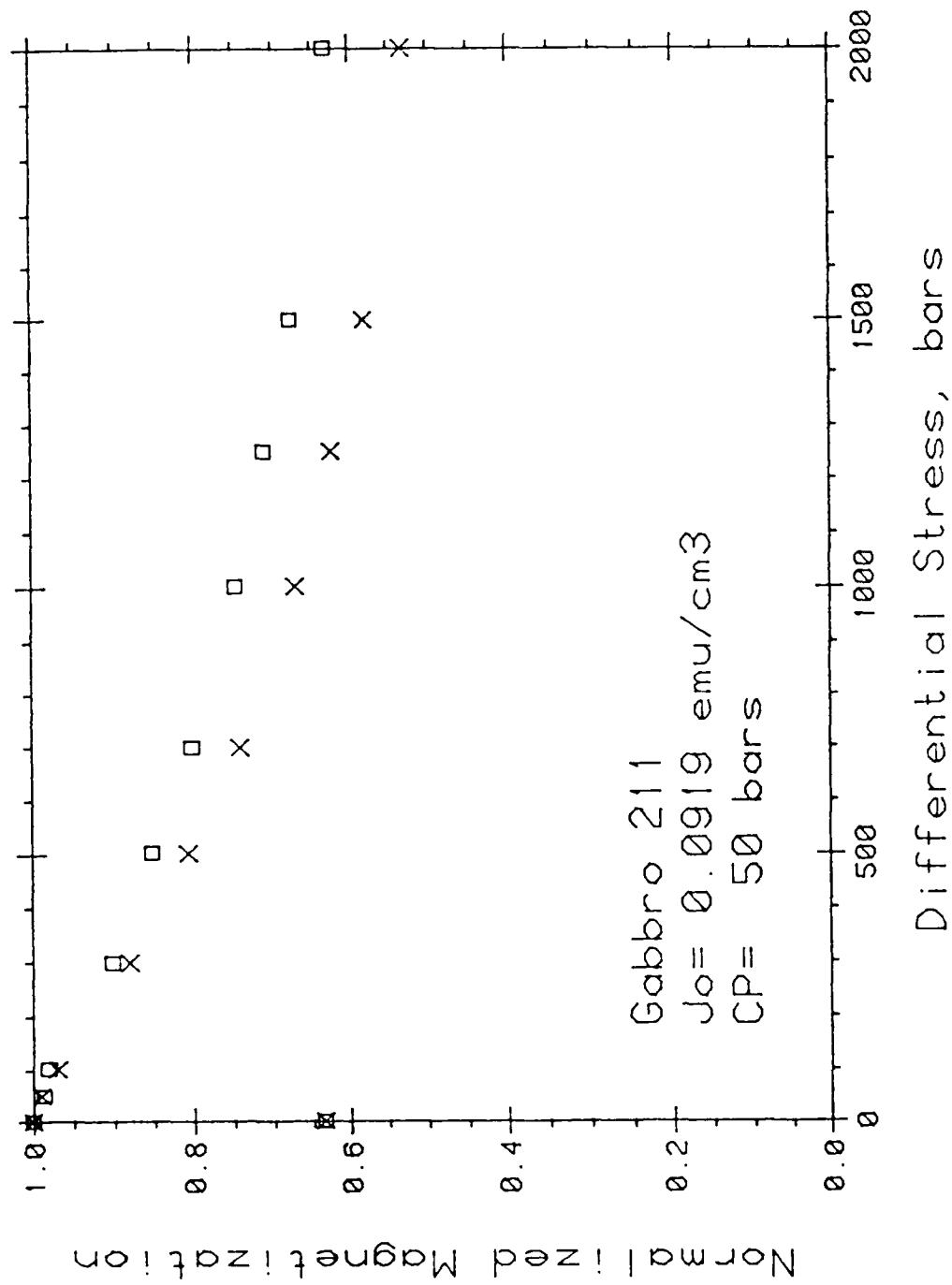


Figure 15. The change in remanent magnetization, normalized to its initial intensity ( $J_0$ ) is plotted as a function of differential stress for a cyclic compression test. The X's represent the observed magnetization at the stress indicated. The squares represent the magnetization at zero differential stress, at the end of the cycle; the data point is plotted at the corresponding differential stress.



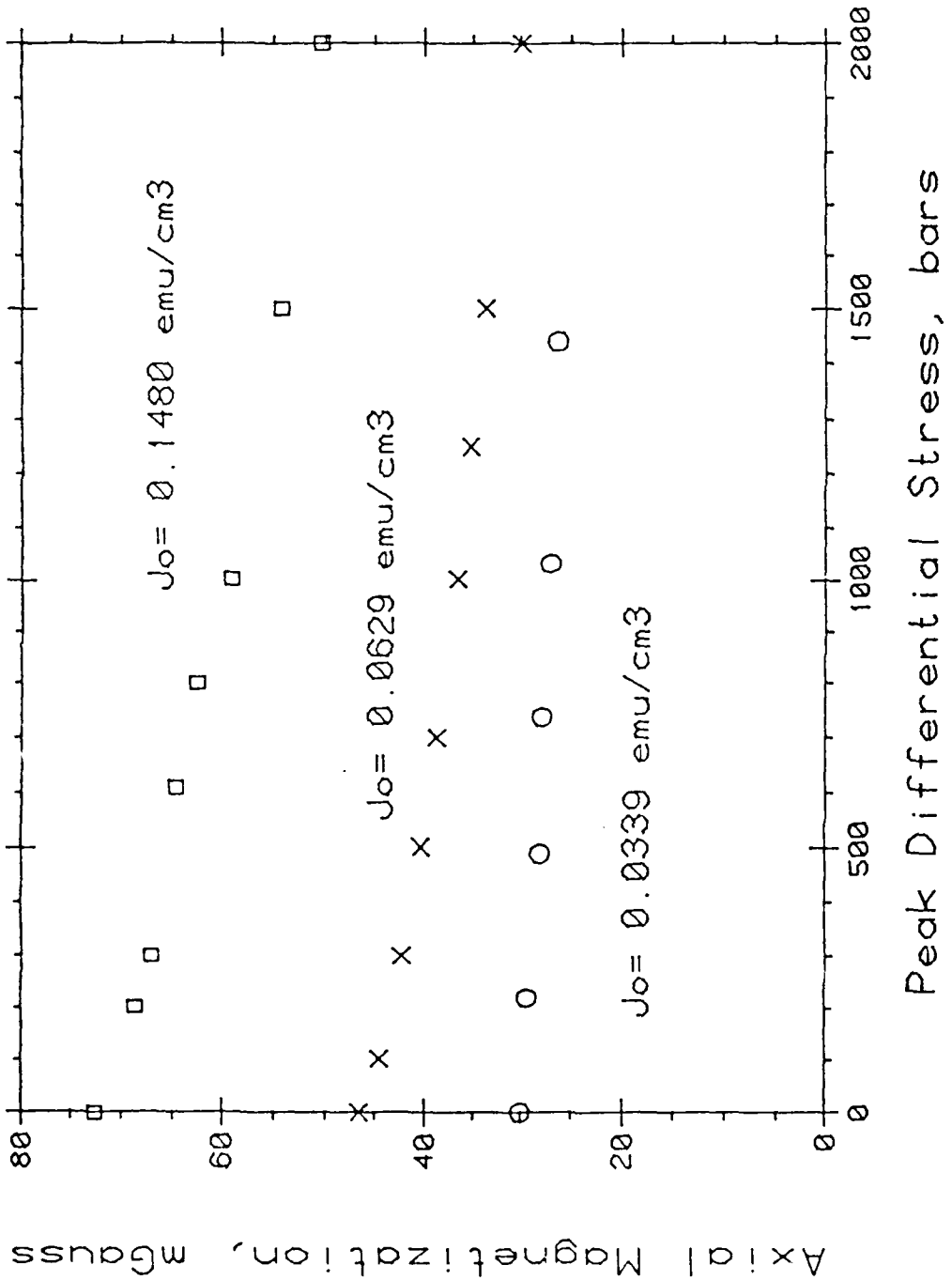


Figure 17. The permanent change in the axial component of remanent magnetization at the termination of a stress cycle (fully unloaded) is plotted as a function of the peak differential stress for the cycle. Results are shown for three gabbro samples with different initial intensities.

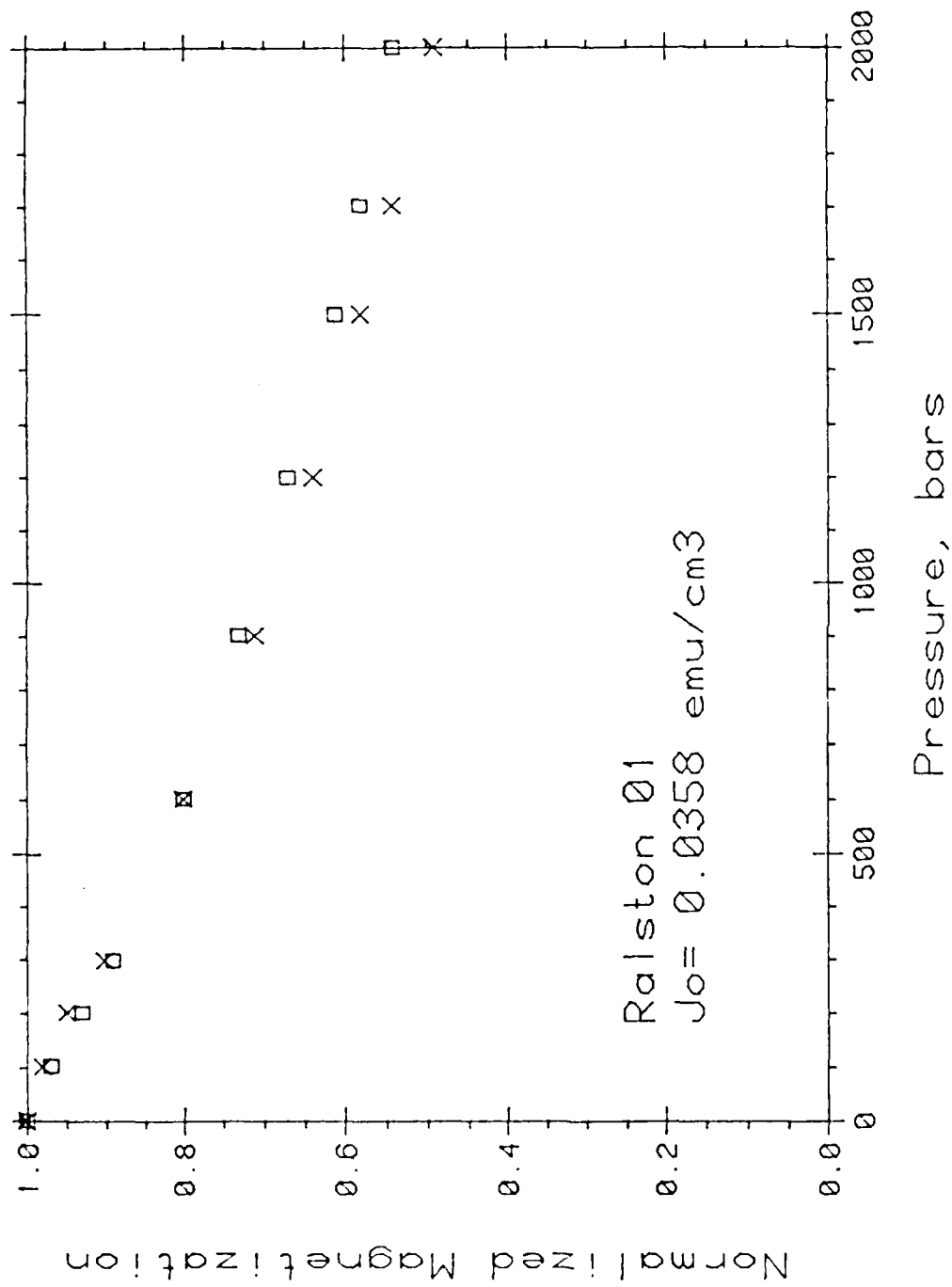


Figure 18a. The change in remanent magnetization, normalized to its initial intensity ( $J_0$ ) is plotted as a function of confining pressure for a cyclic compression test. The X's represent the observed magnetization at the pressure indicated. The squares represent the magnetization at zero pressure, at the end of the cycle; the data point is plotted at the corresponding pressure.

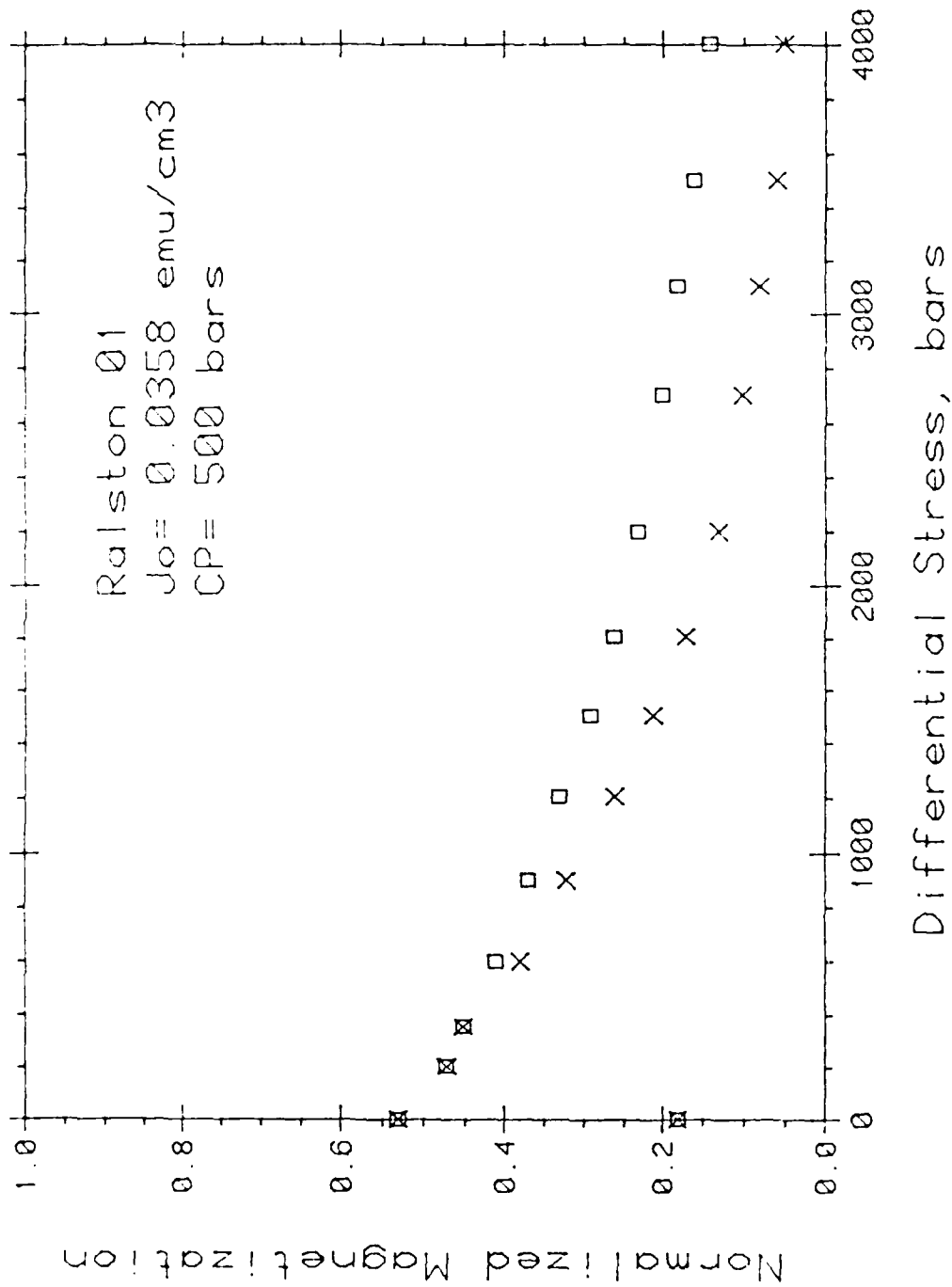


Figure 18b. The change in remanent magnetization, normalized to its initial intensity ( $J_0$ ), is plotted as a function of differential stress at a confining pressure of 500 bars, for cyclic loading. Only the differential stress was reduced to zero at the termination of each cycle. The X's represent the magnetization of the stress indicated. The squares represent the magnetization at zero stress, at the end of the cycle; the data point is plotted at the corresponding peak stress.



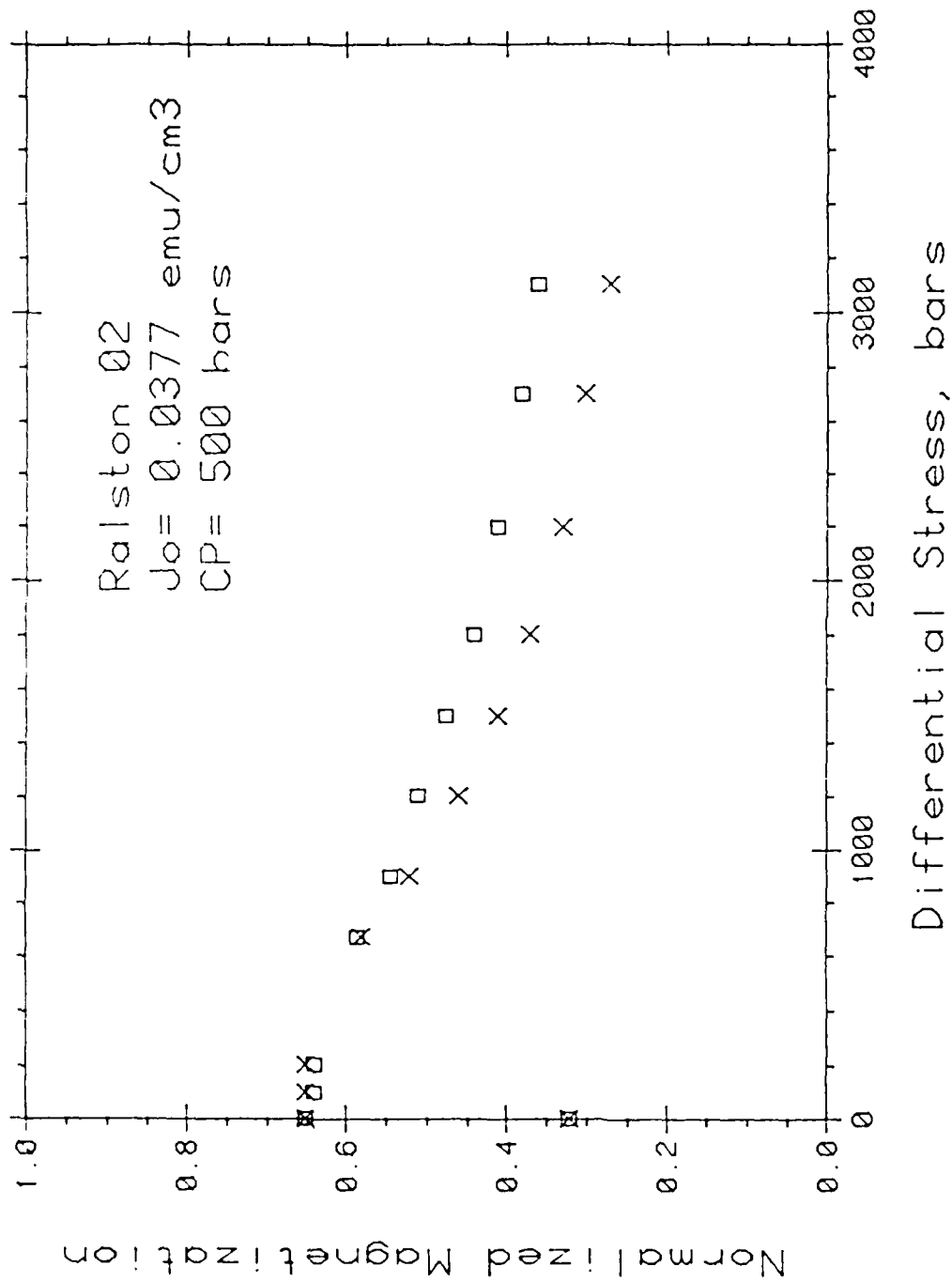


Figure 19b. The change in remanent magnetization, normalized to its initial intensity ( $J_0$ ), is plotted as a function of differential stress at a confining pressure of 500 bars, for cyclic loading. Only the differential stress was reduced to zero at the termination of each cycle. The X's represent the magnetization of the stress indicated. The squares represent the magnetization at zero stress, at the end of the cycle; the data point is plotted at the corresponding peak stress.

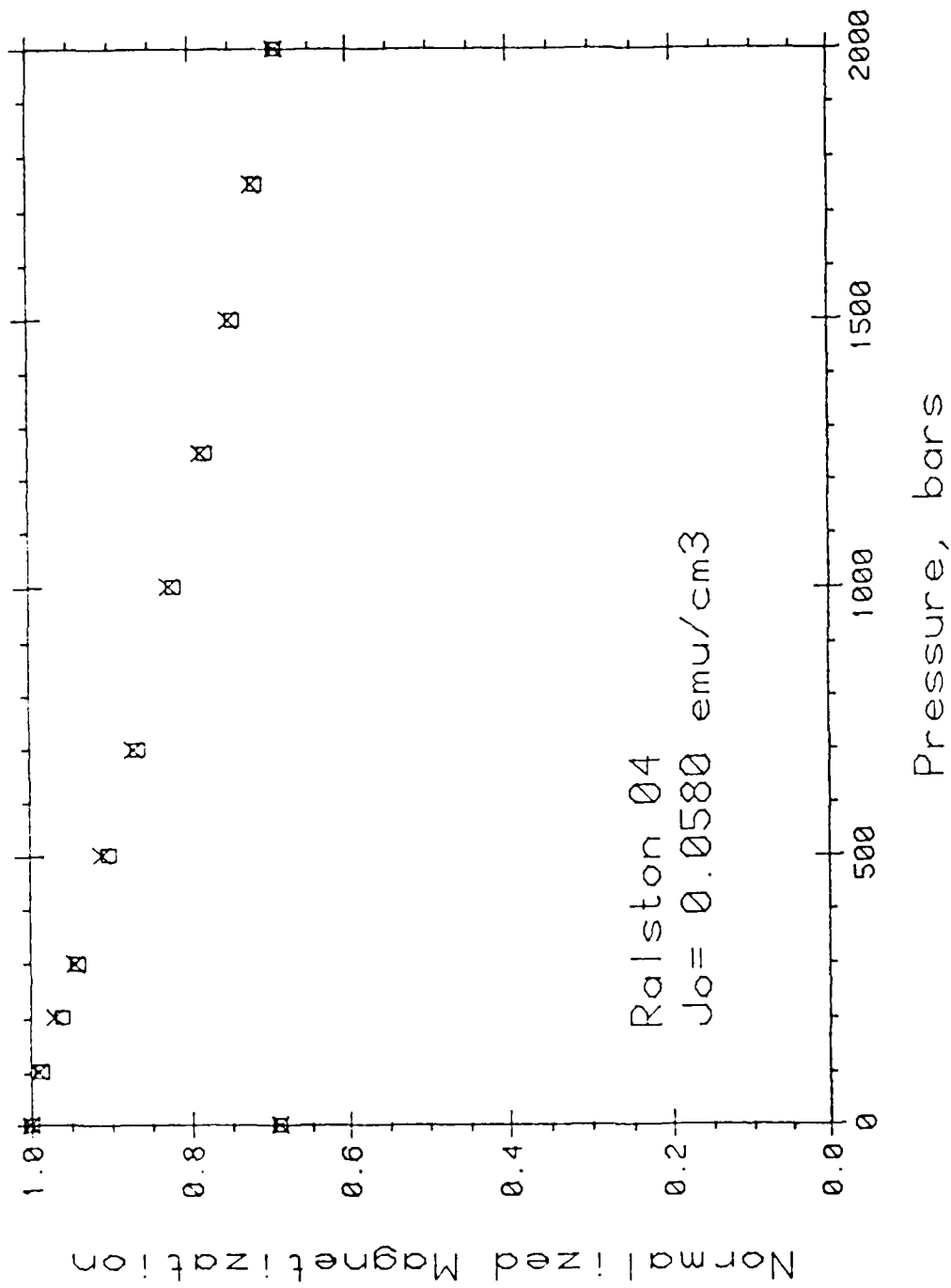


Figure 20 The change in remanent magnetization, normalized to its initial intensity ( $J_0$ ) is plotted as a function of confining pressure for a cyclic compression test. The X's represent the observed magnetization at the pressure indicated. The squares represent the magnetization at zero pressure, at the end of the cycle; the data point is plotted at the corresponding pressure.

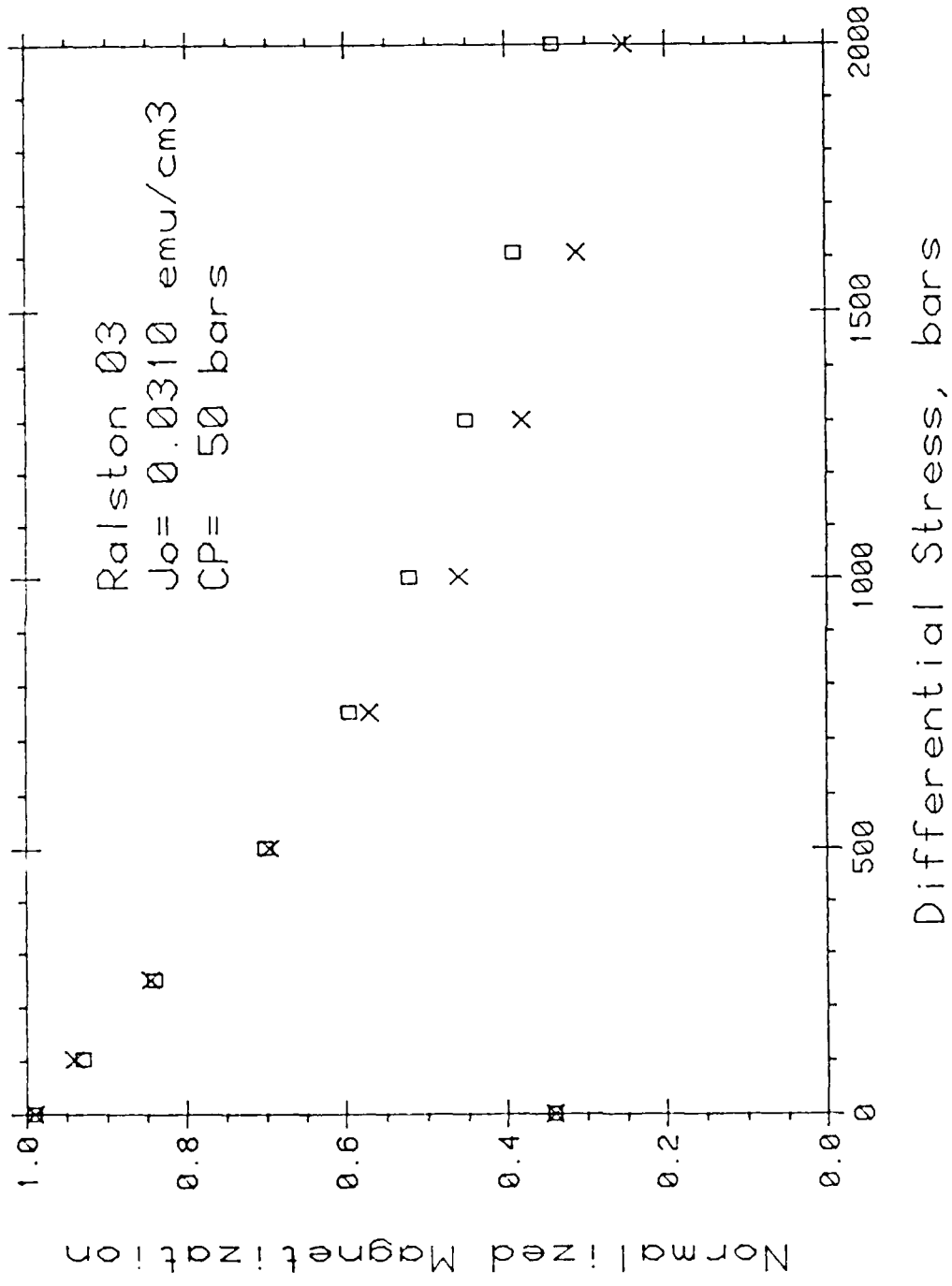


Figure 21a. The change in remanent magnetization, normalized to its initial intensity ( $J_0$ ) is plotted as a function of differential stress for a cyclic compression test. The X's represent the observed magnetization at the stress indicated. The squares represent the magnetization at zero differential stress, at the end of the cycle; the data point is plotted at the corresponding differential stress.

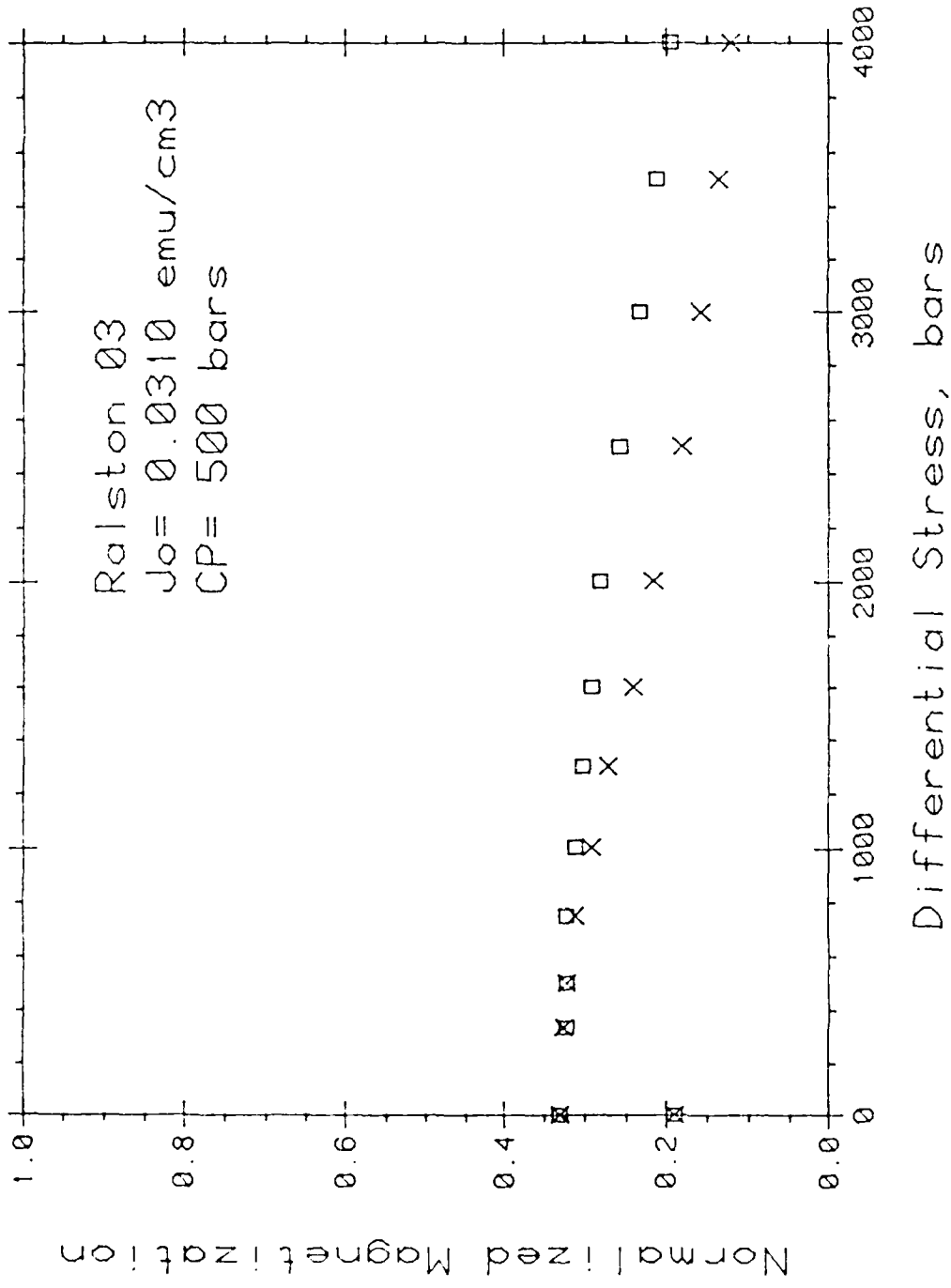


Figure 21b. The change in remanent magnetization, normalized to its initial intensity ( $J_0$ ), is plotted as a function of differential stress at a confining pressure of 500 bars, for cyclic loading. Only the differential stress was reduced to zero at the termination of each cycle. The X's represent the magnetization of the stress indicated. The squares represent the magnetization at zero stress, at the end of the cycle; the data point is plotted at the corresponding peak stress.

END

3-87

DTIC